Author Manuscript Published OnlineFirst on December 13, 2018; DOI: 10.1158/0008-5472.CAN-18-2139
Author manuscripts have been peer reviewed and accepted for publication but have not yet been edited.

Macrophage-derived IL-1β and TNF-α regulate arginine metabolism in neuroblastoma

Livingstone Fultang,[1] Laura D. Gamble,[2] Luciana Gneo,[1] Andrea M. Berry,[3] Sharon A. Egan,[4] Fenna De Bie,[1] Orli Yogev,[5] Georgina L. Eden,[2] Sarah Booth,[1] Samantha Brownhill,[3] Ashley Vardon,[1] Carmel M. McConville,[6] Paul N. Cheng,[7] Murray D. Norris,[2] Heather C. Etchevers,[8] Jayne Murray,[2] David S. Ziegler,[2] Louis Chesler,[5] Ronny Schmidt,[9] Susan A. Burchill,[3] Michelle Haber,[2] Carmela De Santo[†1], Francis Mussai[†*1]

[1]Institute of Immunology and Immunotherapy, University of Birmingham, Birmingham, B15 2TT, UK
[2]Children's Cancer Institute, University of New South Wales, Sydney Australia
[3]Children's Cancer Research Group, Leeds Institute of Cancer and Pathology, University of Leeds, Leeds, LS9 7TF, UK
[4]School of Veterinary Medicine and Science, Sutton Bonington Campus, University of Nottingham, Nottingham, LE12 5RD, UK
[5]The Institute of Cancer Research, London SM2 5MG, UK
[6]Institute of Cancer Genomic Sciences, University of Birmingham, Birmingham, Birmingham, B15 2TT, UK
[7]Bio-Cancer Treatment International, Hong Kong
[8]GMGF, Aix Marseille University, INSERM, U251, Marseille, France
[9]Sciomics GmbH, Heidelberg, Germany

[†] C De Santo and F Mussai contributed equally to this manuscript.

[*] Corresponding author: Francis Mussai, Institute of Immunology and Immunotherapy, University of Birmingham, Birmingham, B15 2TT, United Kingdom. e-mail: francis.mussai@nhs.net. Tel: +44 121 414 7047

The authors have declared that no conflict of interest exists.

Running Title: Macrophage IL-1β/ TNF-α regulate Arginase2

Word Count: 4998

Downloaded from cancerres.aacrjournals.org on January 7, 2019. © 2018 American Association for Cancer Research.

Author Manuscript Published OnlineFirst on December 13, 2018; DOI: 10.1158/0008-5472.CAN-18-2139
Author manuscripts have been peer reviewed and accepted for publication but have not yet been edited.

Abstract

Neuroblastoma is the most common childhood solid tumor, yet the prognosis for high-risk disease remains poor. We demonstrate here that arginase 2 (ARG2) drives neuroblastoma cell proliferation via regulation of arginine metabolism. Targeting arginine metabolism, either by blocking cationic amino acid transporter 1 (CAT-1)-dependent arginine uptake in vitro or therapeutic depletion of arginine by pegylated-recombinant arginase BCT-100, significantly delayed tumor development and prolonged murine survival. Tumor cells polarized infiltrating-monocytes to a M1-macrophage phenotype, which released IL-1β and TNF-α in a RAC-alpha serine/threonine-protein kinase (AKT)-dependent manner. IL-1β and TNF-α established a feedback loop to upregulate ARG2 expression via p38 and extracellular regulated kinases 1/2 (ERK1/2) signalling in neuroblastoma and neural crest-derived cells. Proteomic analysis revealed that enrichment of IL-1β and TNF-α in stage IV human tumor microenvironments was associated with a worse prognosis. These data thus describe an immune-metabolic regulatory loop between tumor cells and infiltrating myeloid cells regulating ARG2, which can be clinically exploited.

Significance

Findings illustrate that cross talk between myeloid cells and tumor cells creates a metabolic regulatory loop that promotes neuroblastoma progression.

Downloaded from cancerres.aacrjournals.org on January 7, 2019. © 2018 American Association for Cancer Research.

Author Manuscript Published OnlineFirst on December 13, 2018; DOI: 10.1158/0008-5472.CAN-18-2139
Author manuscripts have been peer reviewed and accepted for publication but have not yet been edited.

Introduction

The consumption and metabolism of diverse nutrients by cancer cells is recognised as a key regulator of immunity. Glucose metabolism by cancer cells generates a tumour microenvironment that has low levels of glucose, leading to inhibition of T cell cytotoxicity through the accumulation of lactate, microenvironment acidification, and reduced aerobic glycolysis (1-3). Tumour infiltrating monocyte differentiation and cytokine release may be similarly affected, leading to perturbation of their role in coordinating the surrounding immune response (4, 5). Amino acid metabolism also plays a critical role in the function of both normal and malignant cells. Although whole body amino acid homeostasis is regulated through restricted inter-organ enzyme expression, at the cellular level enzyme expression is controlled in the intracellular compartment to maintain metabolic precursor supplies and regulate the wider tissue microenvironment (6).

Arginine is a semi-essential amino acid which is metabolised into ornithine and urea by the expression of cytoplasmic Arginase 1 (ARG1) and mitochondrial Arginase 2 (ARG2), or Nitric Oxide Synthase (NOS) enzymes into reactive nitric oxide species (7). These metabolites feed forward into diverse roles in cell signalling, proliferation and protein synthesis. Cellular breakdown of arginine also plays a critical role in regulating the immune response, a process which has been capitalised on by malignant cells to contribute to their immune escape (8). We recently identified that Acute Myeloid Leukaemias (AML) and neuroblastoma, two of the most common and devastating cancers of childhood create a potent immunosuppressive microenvironment through the expression of ARG2 enzyme which suppresses T-cell immunity (9, 10).

Downloaded from cancerres.aacrjournals.org on January 7, 2019. © 2018 American Association for Cancer Research.

Author Manuscript Published OnlineFirst on December 13, 2018; DOI: 10.1158/0008-5472.CAN-18-2139
Author manuscripts have been peer reviewed and accepted for publication but have not yet been edited.

Although the metabolic effect of cancer cells on shaping the responsiveness of surrounding immune populations is increasingly well described, the reciprocal effects of immune cell populations on modulating cancer cell amino acid metabolism have not previously been reported. In particular the role of arginine metabolism in this process is unknown and the signals which regulate ARG2 in cancer are not well understood. Here we demonstrate how myeloid cells within the tumour microenvironment and tumour cells engage in reciprocal cross-talk to regulate the expression of ARG2 in neuroblastoma cells, and how this arginine metabolism plays a central role in neuroblastoma pathogenesis. Importantly, this study identifies arginine metabolism as a clinically relevant therapeutic target.

Downloaded from cancerres.aacrjournals.org on January 7, 2019. © 2018 American Association for Cancer Research.

Author Manuscript Published OnlineFirst on December 13, 2018; DOI: 10.1158/0008-5472.CAN-18-2139
Author manuscripts have been peer reviewed and accepted for publication but have not yet been edited.

Materials and Methods

Patient Samples

Heparinised blood and tumour samples were obtained from 50 patients with neuroblastoma treated at the Birmingham Children's Hospital and Children's Hospital Oxford. Samples were obtained from patients with newly diagnosed neuroblastoma, at the time of diagnostic biopsy or before the start of treatment. GD2+ neuroblastoma cells were isolated from bone marrow aspirates taken from patients with stage IV disease.

Neuroblastoma murine model

Transgenic Tg(*TH-MYCN*)^{41Waw} mice were genotyped to detect the presence of human *MYCN* transgene or the Chromosome 18 insertion site, using an allelic discrimination methodology (11, 12). Specific assays were designed to measure the presence of the *MYCN* transgene (forward primer 5'-CGACCACAAGGCCCTCAGTA; reverse primer 5'-CAGCCTTGGTGTTGGAGGAG; probe 6FAM-CGCTTCTCCACAGTGACCACGTCG TAMRA; Eurofins) or to the site of the transgene on chromosome 18 which is disrupted during insertion (forward primer 5'- CCACAAAAATATGACTTCCTAAAAGATTT; reverse primer 5'-CATGGGACTTCCTCCTTATATGCT; probe VIC-5'-AACAATTATAACACCATTAGATATG TAMRA). After weaning, *TH-MYCN* mice were palpated for intra-abdominal tumours twice weekly. Mice with palpable tumours ranging in size between 5-20mm in diameter were then humanely sacrificed. At sacrifice, unheparinised and heparinised whole blood, as well as tumour tissue were obtained for further ex vivo analyses. Tumour tissue was processed as

Downloaded from cancerres.aacrjournals.org on January 7, 2019. © 2018 American Association for Cancer Research.

Author Manuscript Published OnlineFirst on December 13, 2018; DOI: 10.1158/0008-5472.CAN-18-2139
Author manuscripts have been peer reviewed and accepted for publication but have not yet been edited.

above. Tumour tissues were stained with anti-mouse GD2 (BioLegend) on ice for 30 minutes. The expression of these markers was then assessed by flow cytometry.

For treatment with BCT-100, mice were treated with 60mg/kg BCT-100 or saline, twice a week, *ip* either from weaning in the prophylaxis setting or upon the development of a 5mm tumour in the treatment setting. Mice were treated until the experimental endpoint of a 10mm abdominal tumour. In the prophylaxis experiment, mice were bled before the start of treatment, midway through the treatment, 24 hours after the fifth dose of either saline or BCT-100, and at tumour endpoint. All experimental protocols were monitored and approved by either The Institute of Cancer Research Animal Welfare and Ethical Review Body, in compliance with guidelines specified by the UK Home Office Animals (Scientific Procedures) Act 1986 and the United Kingdom National Cancer Research Institute guidelines for the welfare of animals in cancer research or the University of New South Wales Animal Care and Ethics Committee and conducted according to the Animal Research Act, 1985 (New South Wales, Australia) and the Australian Code of Practice for Care and Use of Animals for Scientific Purposes (2013).

GD2+ tumour cell and myeloid cell isolation

For isolation of GD2+ tumour cells from human and murine tumours were digested using Type II collagenase, labelled with anti-GD2-PE antibody (BioLegend) and bound to anti-PE coated magnetic beads (Miltenyi Biotec, Bisley, UK). Cells were enriched according to manufacturer's instructions to be >98% GD2+ cells as confirmed by flow cytometry using a PE conjugated anti-human GD2 antibody. For isolation of primary GD2+ cells from the bone marrow of diagnosed stage IV patients, bone marrow aspirates were collected in RPMI 1640 media containing 10%

Downloaded from cancerres.aacrjournals.org on January 7, 2019. © 2018 American Association for Cancer Research.

Author Manuscript Published OnlineFirst on December 13, 2018; DOI: 10.1158/0008-5472.CAN-18-2139
Author manuscripts have been peer reviewed and accepted for publication but have not yet been edited.

FCS. Cells were lysed using erythrocyte lysis buffer (Qiagen) and the white cell fraction isolated by centrifugation. The neuroblastoma cells were labelled with purified mouse anti-human GD2 Clone 14.G2a (BD Pharmingen) and bound to anti-mouse IgG2a/b microbeads (Miltenyi Biotec). Cells were enriched according to manufacturer's instructions (Miltenyi Biotec). For isolation of monocytes, peripheral blood was collected from healthy donors. Monocytes were separated using a Lymphoprep gradient (STEMCELL Technologies) and enriched by positive selection using anti-human CD14 MicroBeads (Miltenyi Biotec).

Cell lines and cultures

Human primary, untransformed, embryonic neural crest (R1113T) or dorsal root and/or sympathetic ganglion-derived stem cells (SZ16) were obtained and cultured as previously described (13-15). Neuroblastoma cell lines (SKNAS, KELLY, IMR-32, LAN-1), the Ewing's sarcoma cell line SKNMC which has high ARG2 expression, and primary GD2+ neuroblastoma cells were cultured in RPMI 1640 medium (Sigma) supplemented with 10% *v/v* foetal bovine serum (FBS, Sigma), 100 U/mL penicillin and streptomycin (Gibco), 1mM sodium pyruvate (Gibco) and 2mM L-Glutamine (Gibco). All cell lines were originally obtained from ATCC and validated for authenticity by DNA short tandem repeats in line with American National Standards Institute ASN-0002-2011 (Northgene). All experiments were performed between passages 3-9, and cells were confirmed as Mycoplasma negative by PCR analysis (LookOut, SIGMA. Latest testing date September 2018). The effects of arginine deprivation were tested on cells cultured in arginine-free RPMI 1640 for SILAC (ThermoFisher Scientific) supplemented with 10% *v/v* arginine-free dialysed FBS (ThermoFisher Scientific). Cells were maintained in an incubator at 5% CO_2 in air and at 37°C.

Downloaded from cancerres.aacrjournals.org on January 7, 2019. © 2018 American Association for Cancer Research.

Author Manuscript Published OnlineFirst on December 13, 2018; DOI: 10.1158/0008-5472.CAN-18-2139
Author manuscripts have been peer reviewed and accepted for publication but have not yet been edited.

Arginase activity assays

The activity of arginase 2 present within cells was determined by measuring the conversion of arginine into urea, as previously described (10).

Antibody microarray analysis

Human stage I neuroblastoma tissue samples (n=13), human stage IV neuroblastoma biopsies (n=9) were analysed using scioDiscover antibody microarrays (Sciomics) which targets 900 cancer-related proteins (16). After sample homogenisation, proteins were extracted with scioExtract buffer (Sciomics) and labelled at an adjusted concentration with scioDye 2 (Sciomics) according to the manufacturer´s instructions. A pool of all protein samples was labelled with scioDye1 and used as a reference for all experiments, allowing competitive dual-colour measurements. Array production, blocking and sample incubation were performed in compliance with strict quality control procedures as reported previously. The arrays were scanned with identical instrument laser power and adjusted PMT setting using a Powerscanner (Tecan). Spot segmentation was performed with the software GenePix Pro 6.0 (Molecular Devices).

Enzyme-linked Immunosorbent Assays (ELISA)

The concentrations of cytokines IFN-γ, IL-1β, TNF-α, TGF-β, IL-6, IL-4, IL-13 and GM-CSF in plasma and cell culture media were measured by sandwich-ELISA kit according to specific manufacturer's instructions.

Downloaded from cancerres.aacrjournals.org on January 7, 2019. © 2018 American Association for Cancer Research.

Author Manuscript Published OnlineFirst on December 13, 2018; DOI: 10.1158/0008-5472.CAN-18-2139
Author manuscripts have been peer reviewed and accepted for publication but have not yet been edited.

Monocyte-driven proliferation assays

Neuroblastoma cells suspended at a density of 1 x 10^6 cells/mL in PBS were labelled with 1µM CellTrace^{TM} FarRed staining solution (Molecular Probes, ThermoFisher Scientific) at 37°C for 20 minutes. Stained cells were washed three times in RPMI-1640 and rested for 10 minutes in complete media. Labelled neuroblastoma cells were then cultured in supernatants from neuroblastoma-induced macrophages (75% final volume), with or without 1µg/mL anti-IL1β (R&D Systems, Catalog #MAB201) and 1ng/mL anti-TNFα (Cell Signalling, Catalog #7321s) neutralising antibodies. Cells were harvested 5 days later and analysed on a CytoFLEX Flow Cytometer (Beckman Coulter). Histograms representing distinct generations of proliferation cells were generated using the FlowJo Software (TreeStar Inc.).

Reverse transcriptase polymerase chain reactions

Total RNA was extracted from cells using either the RNEasy Kit (Qiagen) according to the manufacturer's specifications. Extracted RNA was quantified on a NanoDrop ND-1000 spectrophotometer (ThermoScientific). First strand complimentary DNA (cDNA) was generated by incubating 1µg of extracted RNA with 500ng of random primers (Promega), 0.5mM dNTP (Promega), 1x reverse transcriptase buffer (Promega), 40U RNAse inhibitors (RNAsin, Promega) and either 100U MMLV RNAse H+ or 15U AMV reverse transcriptase (Promega). For endpoint PCR reactions, up to 100ng of sample cDNA was incubated in 5µL of 10X PCR reaction buffer (Invitrogen), 0.5mM dNTPs, one unit of *Taq* polymerase (Invitrogen), 1.5mM $MgCl_2$, 0.5µM of each forward and reverse primer and nuclease free water up to a

Downloaded from cancerres.aacrjournals.org on January 7, 2019. © 2018 American Association for Cancer Research.

Author Manuscript Published OnlineFirst on December 13, 2018; DOI: 10.1158/0008-5472.CAN-18-2139
Author manuscripts have been peer reviewed and accepted for publication but have not yet been edited.

final reaction volume of 50 µL. Human primer sequences are listed in Table S1. All quantitative PCR (RT-qPCR) reactions were conducted on a Fast 7500 real-time PCR thermal cycler (Applied Biosystems).

TaqMan Assays

RNA was isolated using the miRNeasy Mini Kit (Qiagen) and RNA concentration determined by spectrophotometry (NanoDrop 1000, ThermoFisher Scientific). RNA (10 ng per replicate) was reverse transcribed using Superscript™ III Reverse Transcriptase (ThermoFisher Scientific) according to manufacturer's instructions with random hexamer primers (0.3 µg, ThermoFisher Scientific) and RNasin Plus RNase Inhibitor (20 units, Promega). Samples were analysed in triplicate. Samples analysed in the absence of RT enzyme or without RNA were included as negative controls. cDNA was amplified using TaqMan Gene Expression Assays for each target (Table S1, ThermoFisher Scientific) according to manufacturer's instructions. Expression of the housekeeping gene PPIA was determined for each sample using sequence specific reverse and forward primers (200nM forward primer GGACCCAACACAAATGGTTCC, 200nM reverse primer CTTTCACTTTGCCAAACACCA, 100nM FAM labelled probe ATGCTTGCCATCCAACCACTCAGTCTTG). mRNA expression was calculated using the comparative Ct method relative to PPIA. RNA from Cell lines known to express genes of interest were included as control (Table S1)

Study approval

In accordance with the Declaration of Helsinki, patient samples were obtained after written informed consent prior to inclusion in the study. Primary human neural crest-derived stem cell lines were obtained under ethical committee approval PFS14-011 from the French

Downloaded from cancerres.aacrjournals.org on January 7, 2019. © 2018 American Association for Cancer Research.

Author Manuscript Published OnlineFirst on December 13, 2018; DOI: 10.1158/0008-5472.CAN-18-2139
Author manuscripts have been peer reviewed and accepted for publication but have not yet been edited.

Biomedical Agency for the use of embryonic material. Regional Ethics Committee (REC 10/H0501/39) and local hospital trust research approval for the study was granted for United Kingdom hospitals. The Institute of Cancer Research Ethics Committee approved all animal protocols in this study. Collection of diagnostic bone marrow aspirates from Stage IV patients was performed under ethical approval of the Medical Research and Ethics committee (MREC/98/4/023). Procedures were carried out in accordance with UK Home Office Guidelines.

Antibody microarray normalisation and statistical analysis

The acquired raw data were analysed using the linear models for microarray data (LIMMA) package of R-Bioconductor after uploading the median signal intensities. As described previously, a specialised invariant Lowess method was applied for normalisation.(17) For the differential analysis of protein expression, a one-factorial linear model was fitted with LIMMA resulting in a two-sided t-test or F-test based on moderated statistics. Differences in protein abundance between sample groups are presented as log-fold changes (logFC) calculated for the basis 2. The presented p-values were adjusted for multiple testing by controlling the false discovery rate according to Benjamini and Hochberg. In all comparisons, proteins were defined as significantly differential with a log-fold change above 0.5 or below −0.5 and an adjusted p-value below 0.05. Functional enrichment analyses were conducted with the STRING software (https://string-db.org) for the proteins with significantly differential abundance between groups, whereby up- and downregulated proteins were analysed separately.

Downloaded from cancerres.aacrjournals.org on January 7, 2019. © 2018 American Association for Cancer Research.

Author Manuscript Published OnlineFirst on December 13, 2018; DOI: 10.1158/0008-5472.CAN-18-2139
Author manuscripts have been peer reviewed and accepted for publication but have not yet been edited.

Arginase 2 Fluorescence Intensity

Quantification of cell-by-cell fluorescence intensity for Arginase 2 expression across treatment conditions were performed using ImageJ software (National Institute of Health, USA). Briefly confocal image stacks were converted to single channel images. Pixel intensity measurements were determined form single channel Images representing Arginase 2 staining with Image thresholds set to match positive structures within defined cell boundaries.

Statistical analysis

Parametric student t-tests were used to determine the statistical significance of the difference in paired observations between groups (GraphPad Prism, USA). All p values are two-tailed and p values <0.05 were considered to represent statistically significant events. Significance was recorded as * $p<0.05$, ** $p<0.01$, ***$p<0.001$, ****$p<0.0001$.

Downloaded from cancerres.aacrjournals.org on January 7, 2019. © 2018 American Association for Cancer Research.

Author Manuscript Published OnlineFirst on December 13, 2018; DOI: 10.1158/0008-5472.CAN-18-2139
Author manuscripts have been peer reviewed and accepted for publication but have not yet been edited.

Results

Neuroblastoma conditioned macrophages release IL-1β and TNF-α in the tumour microenvironment

Myeloid cells are a major orchestrator of cancer-related inflammation with the potential to support tumour growth, invasion and metastasis. In neuroblastoma we have previously shown a significant increase of immunosuppressive myeloid cells in peripheral blood of patients and in the tumour tissue of the transgenic neuroblastoma TH-MYCN murine model. However the role of intratumoral myeloid cells in human neuroblastoma tumours is not well understood. To understand the landscape inside human tissue at diagnosis, we first investigated the proteomic profile of 23 human neuroblastoma tumours (9 Stage I and 14 Stage IV) using a novel antibody array (18). Non-metric multidimensional scaling from protein array for all analysed samples based on the complete protein expression data revealed separate clustering of Stage I and Stage IV tumours (Figure 1A). Analysis of human neuroblastoma proteomes showed increased expression of the monocyte/macrophage marker CD14 and the granulocytic cell marker CD15 in high stage disease (Figure 1B). Immunohistochemistry of tissue microarrays of 27 tumours, revealed CD14+ cells infiltrated the tumour tissue (Figure 1C upper panels with histoscore Fig 1D, Supp Fig 1A) whilst CD15 staining localised around vasculature (Figure 1C lower panels with histoscore Fig 1D, Supp Fig 1A). Together these findings highlight the potential role of myeloid cells in tumourigenesis.

Monocyte function may be modulated by their environment. To investigate the influence of neuroblastoma tumour cells on monocytes, monocytes enriched from healthy donor blood were co-cultured with sorted Ganglioside G2 (GD2)+ neuroblastoma cells from patients or cell

Downloaded from cancerres.aacrjournals.org on January 7, 2019. © 2018 American Association for Cancer Research.

Author Manuscript Published OnlineFirst on December 13, 2018; DOI: 10.1158/0008-5472.CAN-18-2139
Author manuscripts have been peer reviewed and accepted for publication but have not yet been edited.

lines. We observed that neuroblastoma conditioning led to upregulation of the macrophage marker CD68 and only a minority of cells upregulated CD206 (M2 marker) (Figure 1E and Supp Figures 1B and 1C). In addition, myeloid ARG1 activity was down-regulated (Figure 1F) consistent with polarisation to a M1-phenotype. Importantly immunohistochemistry of neuroblastomas at diagnosis confirmed the infiltration of these CD68+ macrophages within the tumour tissue (Figure 1G and Supp Figure 1D).

Tumour infiltrating myeloid cells can shape the immune response through cytokine release within tumour tissue (19). To investigate the cytokine profile of neuroblastoma induced macrophages, a broad panel of cytokines was analysed in culture supernatants. Tumour-conditioning led to an increased release of IL-1β and TNF-α, with undetectable levels of IL-13, IL-6, IFN-γ, IL-4, TGF-β and GM-CSF consistent with a M1-phenotype (Figure 2A and B, Supp Figure 2A). Tumour cells alone released minimal cytokines (<8 pg/ml, Supp Figure 2B). Although CD15+ granulocytes released IL-8, they did not release either IL-1β or TNF-α following tumour co-culture (Supp Figure 2C). To prove that the release of IL-1β and TNF-α was from the macrophages, intracellular staining for cytokines was performed. Neuroblastoma conditioning led to an increased frequency of IL-1β and TNF-α positive macrophages at 24hours and 48hours (Figure 2C, Supp Figure 3Aand 3B). Using confocal microscopy we confirmed CD14+ cells sorted from patients expressed IL-1β and TNF-α (Supp Figure 3C) and immunohistochemistry of tissue microarrays of 27 tumours confirmed the expression of IL-1β and TNF-α in the tumour-infiltrating macrophages. (Fig 2D; Supp. Figure 4A).

Downloaded from cancerres.aacrjournals.org on January 7, 2019. © 2018 American Association for Cancer Research.

Author Manuscript Published OnlineFirst on December 13, 2018; DOI: 10.1158/0008-5472.CAN-18-2139
Author manuscripts have been peer reviewed and accepted for publication but have not yet been edited.

IL-1β and TNF-α secretion from myeloid cells may be regulated by AKT signalling (20). Co-culture of healthy donor monocytes with neuroblastoma led to AKT phosphorylation(Figure 2E) and AKT inhibition with MK-2206 prevented IL-1β and TNF-α release (Fig 2F and G). No evidence for STAT3, NF-kB, or PI3K pathway activation was identified (Supp Fig 4B). Therefore neuroblastoma cells polarise surrounding monocytes to M1-macrophages which release IL-1β and TNF-α.

Neuroblastoma cell proliferation is dependent on arginine metabolism

Previously we established that that neuroblastoma cells consume arginine from the microenvironment and catabolise this amino acid by ARG2 to create an immunosuppressive microenvironment contributing to immune escape and suboptimal immunotherapy responses (9). However, the role of ARG2 in neuroblastoma development and more widely in human cancers has only received limited study. Arginine metabolism can contribute to cell proliferation. To investigate the role of ARG2 in tumour cell proliferation, we first performed shRNA knock-down for ARG2. ARG2 knock-down led to a significant reduction in cell proliferation (Figure 3A, Supp Figure 4C) confirming the key role of this enzyme. We next blocked uptake of arginine from the microenvironment via Cationic Amino Acid Transporter-1 (CAT1), which we showed is expressed in the majority of neuroblastoma cell lines (Supp Figure 4D). N-nitro-L-arginine (L-NAME) inhibitor led to a significant decrease in tumour cell proliferation (Figure 3B). Culture of tumour cells in the absence of arginine similarly inhibited tumour cell metabolic activity (Figure 3C). BCT-100 is a PEGylated recombinant human arginase that can deplete arginine to undetectable levels in cancer patients leading to clinical

Downloaded from cancerres.aacrjournals.org on January 7, 2019. © 2018 American Association for Cancer Research.

Author Manuscript Published OnlineFirst on December 13, 2018; DOI: 10.1158/0008-5472.CAN-18-2139
Author manuscripts have been peer reviewed and accepted for publication but have not yet been edited.

responses in adult trials (21).Culture of neuroblastoma with BCT-100 led to a rapid inhibition of cell proliferation (Supp Figure 4E), and tumour cell death characterised by PARP cleavage (Supp Figure 5A). Electron microscopy of sorted tumour cells from cell lines and patients confirms loss of cell membrane integrity, and cellular fragmentation (Figure 3D).

To investigate the in vivo dependence of tumour growth on arginine we used the immunocompetent *TH-MYCN* transgenic mouse model which spontaneously develop neuroblastoma tumours .(11) These murine tumour cells also express ARG2 (Supp Figure 5B). We first demonstrated that *ex vivo* treatment of murine GD2+ tumour cells with BCT-100 led to a significant reduction in viable cells (Figure 3E). Treatment of *TH-MYCN* mice with twice-weekly BCT-100 led to a sustained drop in plasma arginine to almost undetectable levels (Figure 3F). To understand if tumour initiation could be delayed or prevented in the absence of arginine, mice were treated prophylactically from the time of weaning at 3 weeks of age, when the tumours were 1-2 mm in size. Neuroblastoma development was significantly delayed and mice survived for significantly longer in the BCT-100 treated group compared to control (p=0.0001, Figure 3G). Following this, we investigated the effect of BCT-100 on established tumours. Here we showed that murine tumour progression was significantly delayed compared to the saline control and overall survival was significantly extended (p=0.0181, Figure 3H). Arginine re-synthesis pathway enzymes ArgininoSuccinate Synthase (ASS) and Ornithine Transcarbamylase (OTC) were not upregulated in GD2+ cells from murine tumours as mechanisms of resistance (Supp Fig 5C). No evidence for BCT-100 drug toxicity in terms of weight or clinical features were identified.

Downloaded from cancerres.aacrjournals.org on January 7, 2019. © 2018 American Association for Cancer Research.

Author Manuscript Published OnlineFirst on December 13, 2018; DOI: 10.1158/0008-5472.CAN-18-2139
Author manuscripts have been peer reviewed and accepted for publication but have not yet been edited.

Macrophage Il-1β and TNF-α drive tumour ARG2 expression via p38/ERK signalling

As ARG2 contributes to tumour cell proliferation, we hypothesised that these macrophage-derived cytokines may reciprocally regulate ARG2 expression. We first showed that the treatment of neuroblastoma cells with low basal expression of ARG2 (SKNAS and IMR32) with IL-1β and TNF-α, either alone or in combination, resulted in upregulated ARG2 expression (Figure 4A and B). Sorted human GD2+ neuroblastoma cells similarly upregulated ARG2 in response to cytokines (Figure 4C).Consistent with this finding, supernatant from tumour-induced macrophages upregulated ARG2 in neuroblastoma cells (Figure 4D, Supp Figure 5D). To investigate whether the M1-macrophages would therefore enhance neuroblastoma cell proliferation via ARG2, we cultured neuroblastoma cells with induced-macrophage supernatants. Supernatants led to increased cell proliferation in neuroblastoma cells (Figure 4E – red) compared to the untreated cells (Figure 4E-black). The phenotype was partially was reversed by the addition of IL-β and TNF-α neutralising antibodies (Figure 4E-green, and Supp Fig 5E).

Neuroblastoma is a pathological derivative of trunk-level neural crest cells, which normally develop into diverse populations including catecholamine-secreting cells of the adrenal medulla, sympathetic, parasympathetic and sensory neurons, and multipotent Schwann cell precursors (22, 23). We hypothesised that a microenvironment containing similar factors to postnatal inflammation may contribute to tumour initiation by upregulating ARG2 in these embryological cells. Analogous to neuroblastoma, treating cultures of normal human embryonic ganglion precursors with IL-1β and TNF-α led to a significant upregulation of

Downloaded from cancerres.aacrjournals.org on January 7, 2019. © 2018 American Association for Cancer Research.

Author Manuscript Published OnlineFirst on December 13, 2018; DOI: 10.1158/0008-5472.CAN-18-2139
Author manuscripts have been peer reviewed and accepted for publication but have not yet been edited.

ARG2 protein expression (Figure 4F), demonstrating the inherent responsiveness of neural crest progenitors to these signals before oncogenic transformation.

We determined that neuroblastoma express the receptors for IL-1β and TNF-α (Figure 5A). The Interleukin 1 Receptor 1 (IL1R1) and Tumour-Necrosis Factor Receptor 1 (TNFR1) receptors can induce a signalling cascade that both converge on a common final effector pathway through ERK1/2 and p38 activation, and Ribosomal Protein S6 Kinase A5 (MSK1) activation (Figure 5B) (24-26). Treatment of neuroblastoma cells with IL-1β and TNF-α leads to NFκB phosphorylation by 0.5 hours and subsequent phosphorylation of ERK1/2 from 1 hour onwards (Figure 5C). Simultaneously, the cytokines also induced p38 phosphorylation at 0.5 hours (Figure 5C). PD98059 binds inactive ERK and prevents phosphorylation and activation by upstream mediators, while SB20308 inhibits p38 catalytic activity but does not affect phosphorylation. The resulting inhibition of p38 or ERK1/2 signalling leads to subsequent downregulation of ARG2 expression in SKNAS neuroblastoma cells (Figure 5D). Blockade of either p38 or ERK1/2 in isolation is insufficient to prevent ARG2 upregulation by cytokines due to compensation by the other side of the pathway (Fig 7B and Supp Fig 5F). MSK1 is at crossroads of the common downstream cascade and can be auto-regulated by kinases including ERK1/2 and p38. SB747651A blockade of MSK1 activity, which is phosphorylated from 0.5 hours onwards (Figure 5C), similarly prevented cytokine-induced ARG2 upregulation (Figure 5E).

Downloaded from cancerres.aacrjournals.org on January 7, 2019. © 2018 American Association for Cancer Research.

Author Manuscript Published OnlineFirst on December 13, 2018; DOI: 10.1158/0008-5472.CAN-18-2139
Author manuscripts have been peer reviewed and accepted for publication but have not yet been edited.

The 1β and TNF-α enriched intra-tumoural microenvironment is associated with high-stage disease

We previously showed that ARG2 expression is highest in Stage IV tumours and is associated with a worse overall survival (9). Cytokines may be functional either within the tumour microenvironment or released into the blood to induce systemic effects. Analysis of blood from 25 neuroblastoma patients at diagnosis revealed that the majority of patients did not have significantly increased TNF-α and IFN-γ compared to healthy controls, although in 9 cases circulating levels of IL-1β and IL-6 were significantly higher (p=0.042) (Figure 6A).

We hypothesised that the intratumoral cytokines driving arginine metabolism in neuroblastoma would promote high stage human neuroblastoma development. To investigate this we further analysed the proteomic profile inside 23 human neuroblastoma tumours. Heat-map representation of protein signals reveal that Stage I and Stage IV tumours show distinct molecular proteomic subgroups, with 7 Stage IV tumours (P21-27) forming a distinct group, while 3 others (P10,P15,P16), had proteomes more similar to Stage I tumours (Figure 6B). Consistent with our in vitro findings, characterisation of the Stage IV tumours identified significantly higher levels of the M1-macrophage derived cytokines IL-1β and TNF-α than Stage I tumours (Figure 6C). In contrast, Stage I tumours had increased expression of the M2-related cytokines TGF-β, IL-10, and IL-4 (Figure 6D). No significant differences in IL-6 and IL-13 expression were identified. Consistent with this, analysis of the expression profile of 88 neuroblastomas (GEOID: GSE16476) revealed high expression of *IL-1β* or *TNF-α* within tumours is associated with a significantly worse overall survival for neuroblastoma patients (p=0.012 and p=0.027 respectively, Figure 7A and B).

Downloaded from cancerres.aacrjournals.org on January 7, 2019. © 2018 American Association for Cancer Research.

Author Manuscript Published OnlineFirst on December 13, 2018; DOI: 10.1158/0008-5472.CAN-18-2139
Author manuscripts have been peer reviewed and accepted for publication but have not yet been edited.

Discussion

Although it is well established that amino acid metabolism can regulate anti-cancer immunity, the capacity of the immune system to regulate cancer amino acid metabolism has rarely been characterised. In this study we identify a key reciprocal regulation between tumour cell arginine metabolism and intra-tumoural macrophages in neuroblastoma. The regulators of ARG2 expression in cancer are poorly understood despite abundant data on its cytoplasmic counterpart ARG1. ARG2 can be upregulated by hypoxia in osteosarcoma cells and non-malignant cells, whilst in pancreatic ductal adenocarcinoma models obesity correlated with increased ARG2 levels and enhanced tumour growth (27, 28)(29, 30). Studies of cytokine regulation of Arginase 2, are limited to non-malignant cells with reports that Th1 or Th2 cytokines have no effects on murine myeloid cells or can modulate ARG2 expression in murine neural stem cells.(31) In humans IL-10 may regulate ARG2 in combination with isoproterenol in macrophages.(32)

We and others have previously reported the ability of neuroblastoma to modulate circulating monocytes into an immunosuppressive phenotype on T cells and NKT cells. (33) Here we demonstrate that the tumour cells also polarise intratumoral monocytes to M1-macrophages, which express and release IL-1β and TNF-α after AKT signal transduction. AKT inhibitors, such as Perifosine, have recently undergone early phase clinical trial development including evaluation in refractory neuroblastoma, with initial results suggesting that targeting this pathway could prolong progression-free survival (34). We show that tumour-polarised macrophages act back to regulate cancer cell arginine metabolism through IL-1β and TNF-α, and drive tumour cell proliferation. Recently murine macrophages were shown to increase

Downloaded from cancerres.aacrjournals.org on January 7, 2019. © 2018 American Association for Cancer Research.

Author Manuscript Published OnlineFirst on December 13, 2018; DOI: 10.1158/0008-5472.CAN-18-2139
Author manuscripts have been peer reviewed and accepted for publication but have not yet been edited.

neuroblastoma proliferation in association with STAT3 phosphorylation, although the factor responsible was not identified.(35) We demonstrate that ARG2 expression is under the control of both p38 and ERK1/2 in human neuroblastoma cells, which lie downstream of the receptors for IL-1β and TNF-α (IL1R1 and TNFR1 respectively). The role of these cytokine pathways in cancer cell expression of ARG2 has not previously been reported. Some redundancy in the signalling cascade is evident, such that inhibition of both receptor pathways, or of their common effect on MSK1, is required to inhibit enzyme expression.

We showed that the Stage IV intratumoural microenvironment is enriched in the expression of IL-1β and TNF-α whilst the converse is true for Stage I tumours. To date, the role of IL-1β and TNF-α in neuroblastoma has primarily centred around the effects of these cytokines on neuroblastoma cell lines used as models of neurodegenerative disease, such as Alzheimer's disease. In terms of its effects on the malignant phenotype, recombinant TNF-α has been shown to be a growth factor for neuroblastoma cell lines, although the mechanism of action was unknown (36). A minor subset of neuroblastoma cells within tumours, may themselves express TNF-α intracellularly or on the cell membrane, but they do not release the cytokine into the microenvironment (33). For IL-1β, little is known in the context of neuroblastoma, although it is reported to drive cyclo-oxygenase (COX-2) expression in neuroblastoma Alzheimer's disease cell line models (37). Importantly, we identified that levels of IL-1β and TNF-α proteins in the plasma are not significantly greater than in healthy donors, indicating that it is the intra-tumoural interactions that are key.

Clinically it is clear that Stage I and Stage IV neuroblastomas are distinct at the levels of tumour dissemination, responses to chemotherapy, and patient outcome. Inter-cellular

Downloaded from cancerres.aacrjournals.org on January 7, 2019. © 2018 American Association for Cancer Research.

Author Manuscript Published OnlineFirst on December 13, 2018; DOI: 10.1158/0008-5472.CAN-18-2139
Author manuscripts have been peer reviewed and accepted for publication but have not yet been edited.

signalling within tumours remains difficult to characterise, although much has been learned from transcriptomic and epigenetic profiling of these tumours (38, 39). The functional interaction of proteins within the cellular ecosystem must be contributing to variation in tumour aggressiveness, although analysis of multiple proteins inside tumours is challenging. To our knowledge, this study is also the first proteomic characterisation of human neuroblastomas at diagnosis and the findings suggest that array-based proteomic profiling can lead to new insights into tumour immunobiology. It has been hypothesised that an immune-stimulatory event, such as infection in early childhood could contribute to the development of childhood cancers either through a normal or aberrant response. Indeed a 'delayed infection' hypothesis had been suggested for childhood acute lymphoblastic leukaemia (40). Although specific infections like Epstein-Barr Virus are directly linked to malignant transformation of cells in Hodgkin's Lymphoma or nasopharyngeal carcinoma, in the majority of paediatric malignancies no evidence of clearly defined cause and effect have been found (41, 42). It is possible that an isolated pro-inflammatory response within a tissue microenvironment could potentially lead to a cytokine profile that drives metabolism in malignant or pre-malignant cells, giving them a survival advantage, allowing development into a frank malignancy. The inflammation could be secondary to very specific infectious agents or an abnormal, pathological response due to immune defects.

Neural crest cells are highly multipotent stem cells in the embryo which give rise to diverse cell types such as melanocytes, odontoblasts, peripheral neurons and support cells, including those of the dorsal root, sympathetic and parasympathetic ganglia, and specific endocrine cells in the thyroid and parathyroid glands and the adrenal medulla(22). We found that neural

Downloaded from cancerres.aacrjournals.org on January 7, 2019. © 2018 American Association for Cancer Research.

Author Manuscript Published OnlineFirst on December 13, 2018; DOI: 10.1158/0008-5472.CAN-18-2139
Author manuscripts have been peer reviewed and accepted for publication but have not yet been edited.

crest-derived primary cells are enriched in ARG2 protein, relative to ARG1. The role of ARG2 in embryological processes is not well understood. Neonatal CD71+ erythroid cells express ARG2, which may affect the response to commensal bacteria in the developing baby, while dendritic cells in the developing foetus also express ARG2 to modulate immune responses *in utero* (43, 44). That the expression of ARG2 in untransformed neural crest-derived stem cells, can be upregulated by immune cytokines IL-1β and TNF-α points to the potential for metabolic changes to occur during malignant transformation or expansion. We have previously shown that AML blasts have similarly upregulated ARG2 in comparison to their non-malignant haematopoietic counterparts (10). Indeed, knock-down of ARG2 significantly reduces the ability of both types of tumour cells to proliferate, suggesting this enzyme provides an advantage to cancer growth and dissemination.

Although arginine metabolism under cytokine control can drive neuroblastoma proliferation, this axis also provides a potential therapeutic target. Targeting tumour-associated myeloid cells has received significant attention to date. Although depletions of myeloid cells can be achieved *in vivo* using anti-GR1 or anti-CR2 antibodies, the effects are very short-lived in mice and no human equivalent exists for clinical translation. One approach to target the feedback loop we have described is to inhibit Il-1β and TNF-α cytokine activity. Anti-TNF-α therapy was the paradigm for anti-cytokine therapies with the development of anti-TNF-α antibody (infliximab) and a decoy anti-TNF-A receptor (etanercept). Although these antibodies have demonstrated remarkable activity in autoimmune conditions, they have only undergone limited study in the setting of cancer therapy. Infliximab has been used as a single agent in

Downloaded from cancerres.aacrjournals.org on January 7, 2019. © 2018 American Association for Cancer Research.

Author Manuscript Published OnlineFirst on December 13, 2018; DOI: 10.1158/0008-5472.CAN-18-2139
Author manuscripts have been peer reviewed and accepted for publication but have not yet been edited.

patients with advanced cancer, with some patients experiencing disease stabilisation (45). The drug has also been trialled to treat renal cell carcinoma and although improvements in immune profiles were noted, there were also significant increases in adverse events (46, 47). Similar antibodies against IL-1β (canakinumab) and its receptor IL-1R1 (anakinra) also exist. Although canakinumab has not been formally tested in patients with an existing cancer, administration of this drug has been shown to significantly reduce incidences of lung cancer and its mortality in patients with atherosclerosis (48). Future combination clinical trials of these agents could represent a novel and potential approach in children with neuroblastoma.

It is now possible to successfully target cancer arginine metabolism through therapeutic arginine depletion with BCT-100, a PEGylated recombinant arginase that induces sustained arginine depletion for months in human trials (49, 50). The drug has completed Phase I/II trials in adult malignancies with an excellent safety profile (21). In this study we demonstrated that BCT-100 not only leads to a decrease in neuroblastoma proliferation with accompanying cell death *in vitro*, but also to delayed progression and prolonged survival in neuroblastoma-bearing mice. These findings support the testing of BCT-100 in an international Phase I/II clinical trial (PARC, NCT03455140) in children with relapsed/refractory malignancies including neuroblastoma. The targeting of both immune and metabolic drivers of tumorigenesis as presented in this study, is rational and clinically achievable, and could be a new paradigm in the treatment of neuroblastoma.

Downloaded from cancerres.aacrjournals.org on January 7, 2019. © 2018 American Association for Cancer Research.

Author Manuscript Published OnlineFirst on December 13, 2018; DOI: 10.1158/0008-5472.CAN-18-2139
Author manuscripts have been peer reviewed and accepted for publication but have not yet been edited.

Acknowledgements

The authors thank the patients and parents who contributed samples to the study as well as Jane Cooper and Cay Shakespeare for obtaining consent and collection of patient samples. We also thank Paul Stanley and Theresa Morris for technical assistance with electron microscopy.

This work was supported by Cancer Research UK, Niayah's Fund, Neuroblastoma UK, Children with Cancer, Treating Children with Cancer, Children's Cancer and Leukaemia Group, the Association Française contre les Myopathies, grants from the National Health and Medical Research Council Australia, Cancer Institute, AKO Foundation, and the alumni and donors to the University of Birmingham.

Downloaded from cancerres.aacrjournals.org on January 7, 2019. © 2018 American Association for Cancer Research.

Author Manuscript Published OnlineFirst on December 13, 2018; DOI: 10.1158/0008-5472.CAN-18-2139
Author manuscripts have been peer reviewed and accepted for publication but have not yet been edited.

References:

1. Angelin A, Gil-de-Gomez L, Dahiya S, Jiao J, Guo L, Levine MH, et al. Foxp3 Reprograms T Cell Metabolism to Function in Low-Glucose, High-Lactate Environments. Cell metabolism. 2017;25(6):1282-93.e7.
2. Calcinotto A, Filipazzi P, Grioni M, Iero M, De Milito A, Ricupito A, et al. Modulation of microenvironment acidity reverses anergy in human and murine tumor-infiltrating T lymphocytes. Cancer Res. 2012;72(11):2746-56.
3. Ho PC, Bihuniak JD, Macintyre AN, Staron M, Liu X, Amezquita R, et al. Phosphoenolpyruvate Is a Metabolic Checkpoint of Anti-tumor T Cell Responses. Cell. 2015;162(6):1217-28.
4. Dietl K, Renner K, Dettmer K, Timischl B, Eberhart K, Dorn C, et al. Lactic acid and acidification inhibit TNF secretion and glycolysis of human monocytes. J Immunol. 2010;184(3):1200-9.
5. Wei G, Twomey D, Lamb J, Schlis K, Agarwal J, Stam RW, et al. Gene expression-based chemical genomics identifies rapamycin as a modulator of MCL1 and glucocorticoid resistance. Cancer Cell. 2006;10(4):331-42.
6. Fultang L, Vardon A, De Santo C, Mussai F. Molecular basis and current strategies of therapeutic arginine depletion for cancer. Int J Cancer. 2016;139(3):501-9.
7. Morris SM, Jr. Arginine Metabolism Revisited. J Nutr. 2016;146(12):2579S-86S.
8. De Santo C, Arscott R, Booth S, Karydis I, Jones M, Asher R, et al. Invariant NKT cells modulate the suppressive activity of IL-10-secreting neutrophils differentiated with serum amyloid A. Nat Immunol. 2010;11(11):1039-46.
9. Mussai F, Egan S, Hunter S, Webber H, Fisher J, Wheat R, et al. Neuroblastoma Arginase Activity Creates an Immunosuppressive Microenvironment That Impairs Autologous and Engineered Immunity. Cancer Res. 2015;75(15):3043-53.
10. Mussai F, De Santo C, Abu-Dayyeh I, Booth S, Quek L, McEwen-Smith RM, et al. Acute myeloid leukemia creates an arginase-dependent immunosuppressive microenvironment. Blood. 2013;122(5):749-58.
11. Weiss W, Aldape K, Mohapatra G, Feuerstein B, Bishop J. Targeted expression of MYCN causes neuroblastoma in transgenic mice. EMBO J. 1997;16(11):2985-95.
12. Haraguchi S, Nakagawara A. A simple PCR method for rapid genotype analysis of the TH-MYCN transgenic mouse. PLoS One. 2009;4(9):e6902.
13. Thomas S, Thomas M, Wincker P, Babarit C, Xu P, Speer MC, et al. Human neural crest cells display molecular and phenotypic hallmarks of stem cells. Human Molecular Genetics. 2008;17(21):3411-25.
14. de Pontual L, Zaghloul NA, Thomas S, Davis EE, McGaughey DM, Dollfus H, et al. Epistasis between RET and BBS mutations modulates enteric innervation and causes syndromic Hirschsprung disease. Proceedings of the National Academy of Sciences of the United States of America. 2009;106(33):13921-6.
15. Boeva V, Louis-Brennetot C, Peltier A, Durand S, Pierre-Eugène C, Raynal V, et al. Heterogeneity of neuroblastoma cell identity defined by transcriptional circuitries. Nature Genetics. 2017;49:1408.
16. Schroder C, Srinivasan H, Sill M, Linseisen J, Fellenberg K, Becker N, et al. Plasma protein analysis of patients with different B-cell lymphomas using high-content antibody microarrays. Proteomics Clin Appl. 2013;7(11-12):802-12.
17. Sill M, Schroder C, Hoheisel JD, Benner A, Zucknick M. Assessment and optimisation of normalisation methods for dual-colour antibody microarrays. BMC Bioinformatics. 2010;11:556.

Downloaded from cancerres.aacrjournals.org on January 7, 2019. © 2018 American Association for Cancer Research.

Author Manuscript Published OnlineFirst on December 13, 2018; DOI: 10.1158/0008-5472.CAN-18-2139
Author manuscripts have been peer reviewed and accepted for publication but have not yet been edited.

18. Ruiz-Babot G, Balyura M, Hadjidemetriou I, Ajodha SJ, Taylor DR, Ghataore L, et al. Modeling Congenital Adrenal Hyperplasia and Testing Interventions for Adrenal Insufficiency Using Donor-Specific Reprogrammed Cells. Cell Rep. 2018;22(5):1236-49.
19. Engblom C, Pfirschke C, Pittet MJ. The role of myeloid cells in cancer therapies. Nat Rev Cancer. 2016;16(7):447-62.
20. Xie S, Chen M, Yan B, He X, Chen X, Li D. Identification of a role for the PI3K/AKT/mTOR signaling pathway in innate immune cells. PLoS One. 2014;9(4):e94496.
21. Yau T, Cheng PN, Chan P, Chen L, Yuen J, Pang R, et al. Preliminary efficacy, safety, pharmacokinetics, pharmacodynamics and quality of life study of pegylated recombinant human arginase 1 in patients with advanced hepatocellular carcinoma. Invest New Drugs. 2015;33(2):496-504.
22. Le Douarin N, Kalcheim C. The neural crest. 2nd ed. Cambridge, UK ; New York, NY, USA: Cambridge University Press; 1999. xxiii, 445 p. p.
23. Espinosa-Medina I, Outin E, Picard CA, Chettouh Z, Dymecki S, Consalez GG, et al. Neurodevelopment. Parasympathetic ganglia derive from Schwann cell precursors. Science. 2014;345(6192):87-90.
24. Turner MD, Nedjai B, Hurst T, Pennington DJ. Cytokines and chemokines: At the crossroads of cell signalling and inflammatory disease. Biochim Biophys Acta. 2014;1843(11):2563-82.
25. Campbell J, Ciesielski CJ, Hunt AE, Horwood NJ, Beech JT, Hayes LA, et al. A Novel Mechanism for TNF- Regulation by p38 MAPK: Involvement of NF- B with Implications for Therapy in Rheumatoid Arthritis. The Journal of Immunology. 2004;173(11):6928-37.
26. Qin J, Jiang Z, Qian Y, Casanova JL, Li X. IRAK4 kinase activity is redundant for interleukin-1 (IL-1) receptor-associated kinase phosphorylation and IL-1 responsiveness. J Biol Chem. 2004;279(25):26748-53.
27. Talavera MM, Nuthakki S, Cui H, Jin Y, Liu Y, Nelin LD. Immunostimulated Arginase II Expression in Intestinal Epithelial Cells Reduces Nitric Oxide Production and Apoptosis. Front Cell Dev Biol. 2017;5:15.
28. Xue J, Nelin LD, Chen B. Hypoxia induces arginase II expression and increases viable human pulmonary artery smooth muscle cell numbers via AMPKalpha1 signaling. Am J Physiol Lung Cell Mol Physiol. 2017;312(4):L568-L78.
29. Setty BA, Pillay Smiley N, Pool CM, Jin Y, Liu Y, Nelin LD. Hypoxia-induced proliferation of HeLa cells depends on epidermal growth factor receptor-mediated arginase II induction. Physiol Rep. 2017;5(6).
30. Zaytouni T, Tsai PY, Hitchcock DS, DuBois CD, Freinkman E, Lin L, et al. Critical role for arginase 2 in obesity-associated pancreatic cancer. Nat Commun. 2017;8(1):242.
31. Munder M, Eichmann K, Moran M, Centeno F, Soler G, Modolell M. Th1/Th2-regulated expression of arginase isoforms in murine macrophages and dendritic cells. Journal of Immunology. 1999;163(7):3771-7.
32. Barksdale AR, Bernard AC, Maley ME, Gellin GL, Kearney PA, Boulanger BR, et al. Regulation of arginase expression by T-helper II cytokines and isoproterenol. Surgery. 2004;135(5):527-35.
33. Liu D, Song L, Wei J, Courtney AN, Gao X, Marinova E, et al. IL-15 protects NKT cells from inhibition by tumor-associated macrophages and enhances antimetastatic activity. J Clin Invest. 2012;122(6):2221-33.
34. Kushner BH, Cheung NV, Modak S, Becher OJ, Basu EM, Roberts SS, et al. A phase I/Ib trial targeting the Pi3k/Akt pathway using perifosine: Long-term progression-free survival of patients with resistant neuroblastoma. Int J Cancer. 2017;140(2):480-4.
35. Hadjidaniel M, Muthugounder S, Hung L, Sheard M, Shirinbak S, Chan R, et al. Tumor-associated macrophages promote neuroblastoma via STAT3 phosphorylation and up-regulation of c-MYC. Oncotarget. 2017;8(53):91516-29.

Downloaded from cancerres.aacrjournals.org on January 7, 2019. © 2018 American Association for Cancer Research.

Author Manuscript Published OnlineFirst on December 13, 2018; DOI: 10.1158/0008-5472.CAN-18-2139
Author manuscripts have been peer reviewed and accepted for publication but have not yet been edited.

36. Goillot E, Combaret V, Ladenstein R, Baubet D, Blay JY, Philip T, et al. Tumor necrosis factor as an autocrine growth factor for neuroblastoma. Cancer Research. 1992;52(11):3194-200.
37. Fiebich B, Mueksch B, Boehringer M, Hull M. Interleukin-1beta induces cyclooxygenase-2 and prostaglandin E(2) synthesis in human neuroblastoma cells: involvement of p38 mitogen-activated protein kinase and nuclear factor-kappaB. J Neurochem. 2000;75(5):2020-8.
38. Henrich KO, Bender S, Saadati M, Dreidax D, Gartlgruber M, Shao C, et al. Integrative Genome-Scale Analysis Identifies Epigenetic Mechanisms of Transcriptional Deregulation in Unfavorable Neuroblastomas. Cancer Res. 2016;76(18):5523-37.
39. van Groningen T, Koster J, Valentijn LJ, Zwijnenburg DA, Akogul N, Hasselt NE, et al. Neuroblastoma is composed of two super-enhancer-associated differentiation states. Nat Genet. 2017;49(8):1261-6.
40. Greaves M. Infection, immune responses and the aetiology of childhood leukaemia. Nat Rev Cancer. 2006;6(3):193-203.
41. Schmidt LS, Kamper-Jorgensen M, Schmiegelow K, Johansen C, Lahteenmaki P, Trager C, et al. Infectious exposure in the first years of life and risk of central nervous system tumours in children: analysis of birth order, childcare attendance and seasonality of birth. Br J Cancer. 2010;102(11):1670-5.
42. Hwee J, Tait C, Sung L, Kwong JC, Sutradhar R, Pole JD. A systematic review and meta-analysis of the association between childhood infections and the risk of childhood acute lymphoblastic leukaemia. Br J Cancer. 2018;118(1):127-37.
43. Elahi S, Ertelt JM, Kinder JM, Jiang TT, Zhang X, Xin L, et al. Immunosuppressive CD71+ erythroid cells compromise neonatal host defence against infection. Nature. 2013;504(7478):158-62.
44. McGovern N, Shin A, Low G, Low D, Duan K, Yao LJ, et al. Human fetal dendritic cells promote prenatal T-cell immune suppression through arginase-2. Nature. 2017;546(7660):662-6.
45. Brown ER, Charles KA, Hoare SA, Rye RL, Jodrell DI, Aird RE, et al. A clinical study assessing the tolerability and biological effects of infliximab, a TNF-alpha inhibitor, in patients with advanced cancer. Ann Oncol. 2008;19(7):1340-6.
46. Larkin JM, Ferguson TR, Pickering LM, Edmonds K, James MG, Thomas K, et al. A phase I/II trial of sorafenib and infliximab in advanced renal cell carcinoma. Br J Cancer. 2010;103(8):1149-53.
47. Harrison ML, Obermueller E, Maisey NR, Hoare S, Edmonds K, Li NF, et al. Tumor necrosis factor alpha as a new target for renal cell carcinoma: two sequential phase II trials of infliximab at standard and high dose. J Clin Oncol. 2007;25(29):4542-9.
48. Ridker PM, MacFadyen JG, Thuren T, Everett BM, Libby P, Glynn RJ, et al. Effect of interleukin-1β inhibition with canakinumab on incident lung cancer in patients with atherosclerosis: exploratory results from a randomised, double-blind, placebo-controlled trial. The Lancet. 2017;390(10105):1833-42.
49. Yau T, Cheng PN, Chan P, Chan W, Chen L, Yuen J, et al. A phase 1 dose-escalating study of pegylated recombinant human arginase 1 (Peg-rhArg1) in patients with advanced hepatocellular carcinoma. Invest New Drugs. 2013;31(1):99-107.
50. De Santo C, Cheng P, Beggs A, Egan S, Bessudo A, Mussai F. Metabolic therapy with PEG-arginase induces a sustained complete remission in immunotherapy-resistant melanoma. J Hematol Oncol. 2018;11(1):68.

Downloaded from cancerres.aacrjournals.org on January 7, 2019. © 2018 American Association for Cancer Research.

Author Manuscript Published OnlineFirst on December 13, 2018; DOI: 10.1158/0008-5472.CAN-18-2139
Author manuscripts have been peer reviewed and accepted for publication but have not yet been edited.

Figure Legends

Figure 1: Neuroblastoma induces M1-macrophages

A) Non-metric multi-dimension scaling of Stage I (RED) and Stage IV (BLUE) tumours at diagnosis shows distinct proteomic profiles for these two stages of tumours B) Proteomic analysis of Stage I and IV tumours identifies significantly higher expression of CD14 and CD15 in Stage IV tumours C) Immunohistochemical staining of sections from neuroblastomas showing infiltration of CD14+ (upper) and CD15+(lower) myeloid cells. Representative sections shown of n=27, tissue microarray D) Histoscores of CD14 and CD15 staining in neuroblastoma tissue microarrays of n=27 tumours E) CD14+ monocytes from healthy donors co-cultured with sorted GD2+ tumour cells from patients upregulate CD68 expression (upper). Minimal CD206 upregulation was seen. Representative flow cytometry shown (n=5) F) CD14+ monocytes from healthy donors co-cultured with neuroblastoma have decreased arginase activity, as assessed by conversion of ornithine to urea in a colorimetric assay. (n=3) G) Immunohistochemical staining of sections from neuroblastomas showing infiltration of CD68+ macrophages. Representative sections shown of n=27, tissue microarray

Figure 2: Tumour-induced macrophages cells release IL-1β and TNF-α through p-AKT signalling

ELISA of supernatants following co-culture of healthy donor monocytes with neuroblastoma cell lines, showing increased IL-1β (A) and TNF-α (B) (n=7) C) Co-culture of monocytes from healthy donors with tumour cell lines for 48hours leads to upregulation of IL-1β and TNF-α expression, compared to those cultured in RPMI10% media. Flow cytometry staining shown, gated on CD14+ cells. Representative staining from 3 independent experiments D)

Downloaded from cancerres.aacrjournals.org on January 7, 2019. © 2018 American Association for Cancer Research.

Author Manuscript Published OnlineFirst on December 13, 2018; DOI: 10.1158/0008-5472.CAN-18-2139
Author manuscripts have been peer reviewed and accepted for publication but have not yet been edited.

Immunohistochemical staining of sections from neuroblastomas showing infiltration of CD33+IL-1β+ and CD33+TNF-α+ macrophages. Representative sections from n=27 TMA shown E) CD14+ myeloid cells from healthy donors were sorted following co-culture with neuroblastoma cell lines. Co-culture leads to increased expression of p-AKT, as shown by Western blotting (n=3) Addition of AKT inhibitor MK2206 to co-cultures of CD14+ cells and neuroblastoma cell lines leads to inhibition of IL-1β (F) and TNF-α (G) release (n=3) protein expression.

Figure 3: Neuroblastoma proliferation is dependent on arginine metabolism

A) shRNA knock-out of *ARG2* in SKNMC (high baseline ARG2 expression) decreases cell proliferation. Fold change in cell number after 72h compared to baseline. Experiment performed in duplicate. Corresponding Western blots for ARG2 in wild-type and knock-down cell lines shown below, with actin as a loading control B) Proliferation of tumour cell lines is inhibited by CAT1 inhibition with L-NAME, measured by ^{3}H-thymidine incorporation after 72 hours C) Cell lines were cultured with RPMI+10%FBS (R10%) or arginine-free RPMI+10%FBS (R10%-arginine). Metabolic activity was measured by MTT after 72h. n=7 replicates D) Sorted GD2+ neuroblastoma cells from patients were treated with BCT-100 (600ng/mL). Analysis of cell death was performed by transmission electron microscopy (Representative micrographs of 2 out of 6 patients shown). Upper panel show untreated cells. Lower panels show post treatment with 600ng/mL BCT-100. Features consistent with organelle enlargement, cell membrane permeablisation, and cellular fragmentation with 600ng/mL BCT-100. Experiments performed on 3 separate occasions E) Sorted GD2+ cells from TH-MYCN murine neuroblastomas were cultured with BCT-100 (600ng/mL) for 72 hours. The percentage of

Downloaded from cancerres.aacrjournals.org on January 7, 2019. © 2018 American Association for Cancer Research.

Author Manuscript Published OnlineFirst on December 13, 2018; DOI: 10.1158/0008-5472.CAN-18-2139
Author manuscripts have been peer reviewed and accepted for publication but have not yet been edited.

viable cells relative to untreated controls was determined by flow cytometry, using propidium iodide staining. BCT-100 leads to a decrease in murine neuroblastoma cell viability *ex vivo* F) Plasma from control (saline) and BCT-100 treated TH-MYCN mice was collected at the start (PRE), 16 days after (MID), and at tumour end-point (END). The concentration of arginine was determined by ELISA. BCT-100 maintains a significant reduction in the plasma arginine concentration *in vivo*. n=6 G) TH-MYCN mice were treated with BCT-100 (60mg/kg) twice weekly intraperitoneally (*ip*) from the time of weaning at 3 weeks of age before overt tumour formations (Prophylaxis). Kaplan-Meier curves show that the development of tumours is significantly delayed, and that survival is increased in BCT-100 treated mice H) TH-MYCN mice were treated with BCT-100 (60mg/kg) twice weekly *ip* once 5 mm tumours were palpable (Treatment). Kaplan-Meier curves show a significant prolongation of survival in BCT-100 treated mice.

Figure 4: Il-1β and TNF-α upregulate Arginase 2 expression and tumour cell proliferation

Treatment of neuroblastoma cells SKNAS (A) and IMR32 (B) with recombinant cytokines alone or in combination leads to upregulation of ARG2, measured by western blot. Actin is shown as a loading control. Corresponding densitometry of ARG2 relative to actin shown. Representative of n=6 replicates C) Treatment of sorted GD2+ primary neuroblastoma cells (Patient 53 and Patient 54) with cytokines leads to upregulation of *ARG2*, measured by Western blot. Actin is shown as a loading control. Corresponding densitometry of *ARG2* relative to actin shown D) Representative confocal microscopy of neuroblastoma cell line SKNAS shows expression of arginase 2 is increased following culture with the supernatants of neuroblastoma-induced macrophages. DAPI – blue, ARG2 – green, MitoTracker – red (n=3) E)

Downloaded from cancerres.aacrjournals.org on January 7, 2019. © 2018 American Association for Cancer Research.

Author Manuscript Published OnlineFirst on December 13, 2018; DOI: 10.1158/0008-5472.CAN-18-2139
Author manuscripts have been peer reviewed and accepted for publication but have not yet been edited.

Neuroblastoma cell proliferation is enhanced in the presence of neuroblastoma-induced macrophage conditioned supernatants (MCM). The addition of anti-TNFα and IL-1β antibodies (inhibitors) reversed the proliferative effects of MCM. Cell proliferation of neuroblastoma shown by dilution of Cell Trace reagent, measured by flow cytometry F) Treatment of embryonic dorsal root ganglion stem cell line SZ16 with recombinant cytokines alone or in combination leads to upregulation of ARG2, as measured by Western blot. Actin is shown as a loading control. Corresponding densitometry of ARG2 relative to actin shown. Representative of n=3 replicates.

Figure 5: Il-1β and TNF-α drive Arginase 2 expression in a p38/ERK dependent manner

A) Neuroblastoma cell lines express the IL-1b and TNF-a receptors on the cell surface as assessed by flow cytometry. (n=3) B) Schematic showing the signalling pathway for IL-1β and TNF-α cytokines, via ERK1/2, p38 and MSK1 C) Time course (hours) in which IL-1β and TNF-α lead to increased p-NFκB (0.5 hours), p-ERK1/2 (from 1 hour onwards), p-p38 (0.5 hours) and p-MSK1 (0.5 hours onwards). ERK1/2, p38, and MSK1 activity are inhibited by PD90859, SB203508, and SB747651A respectively. Western blot shown. Representative of n=3 replicates D) Treatment of SKNAS neuroblastoma cells with recombinant cytokines leads to upregulation of ARG2, which is inhibited by ERK1/2 and p38 inhibition. Western blot shown with actin as a loading control. Corresponding densitometry of ARG2 relative to actin shown N=3 replicates E) Treatment of SKNAS neuroblastoma cells with recombinant cytokines leads to upregulation of ARG2, which is inhibited by MSK1 inhibition. Western blot shown with actin as a loading control. Corresponding densitometry of ARG2 relative to actin shown n=3 replicates

Downloaded from cancerres.aacrjournals.org on January 7, 2019. © 2018 American Association for Cancer Research.

Author Manuscript Published OnlineFirst on December 13, 2018; DOI: 10.1158/0008-5472.CAN-18-2139
Author manuscripts have been peer reviewed and accepted for publication but have not yet been edited.

Figure 6: The Stage IV neuroblastoma intratumoural microenvironment is enriched in IL-1β and TNFα A)ELISA Quantification of cytokine titres in neuroblastoma patient plasma (n=26) at diagnosis identifies no significant differences in circulating levels of TNF-α and IFN-γ. Circulating IL-1β concentrations were significantly higher in some patients at diagnosis. B) Heatmap of Stage I (RED) and Stage IV (BLUE) tumours at diagnosis shows distinct proteomic profiles for these two stages of tumours C) Proteomic analysis of Stage I and IV tumours at diagnosis identifies significantly higher expression of the IL-1β, TNF-α, as well as IFN-γ in Stage IV tumours D) Stage I tumours express significantly higher Th2 cytokines TGF-β, IL-10, and IL-4 by proteomic analysis

Figure 7: High IL-1β or TNF-α expression in tumours correlate with a worse overall survival for patients Kaplan-Meier curves of n=88 neuroblastoma patients at diagnosis identifying high IL-1β (A) or TNF-α (B) expression in tumours is associated with a worse overall survival. All data are analysed in accordance with the public Versteeg database 'R2: microarray analysis and visualization platform' (http://r2.aml.nl).

Downloaded from cancerres.aacrjournals.org on January 7, 2019. © 2018 American Association for Cancer Research.

Author Manuscript Published OnlineFirst on December 13, 2018; DOI: 10.1158/0008-5472.CAN-18-2139
Author manuscripts have been peer reviewed and accepted for publication but have not yet been edited.

Figure 1

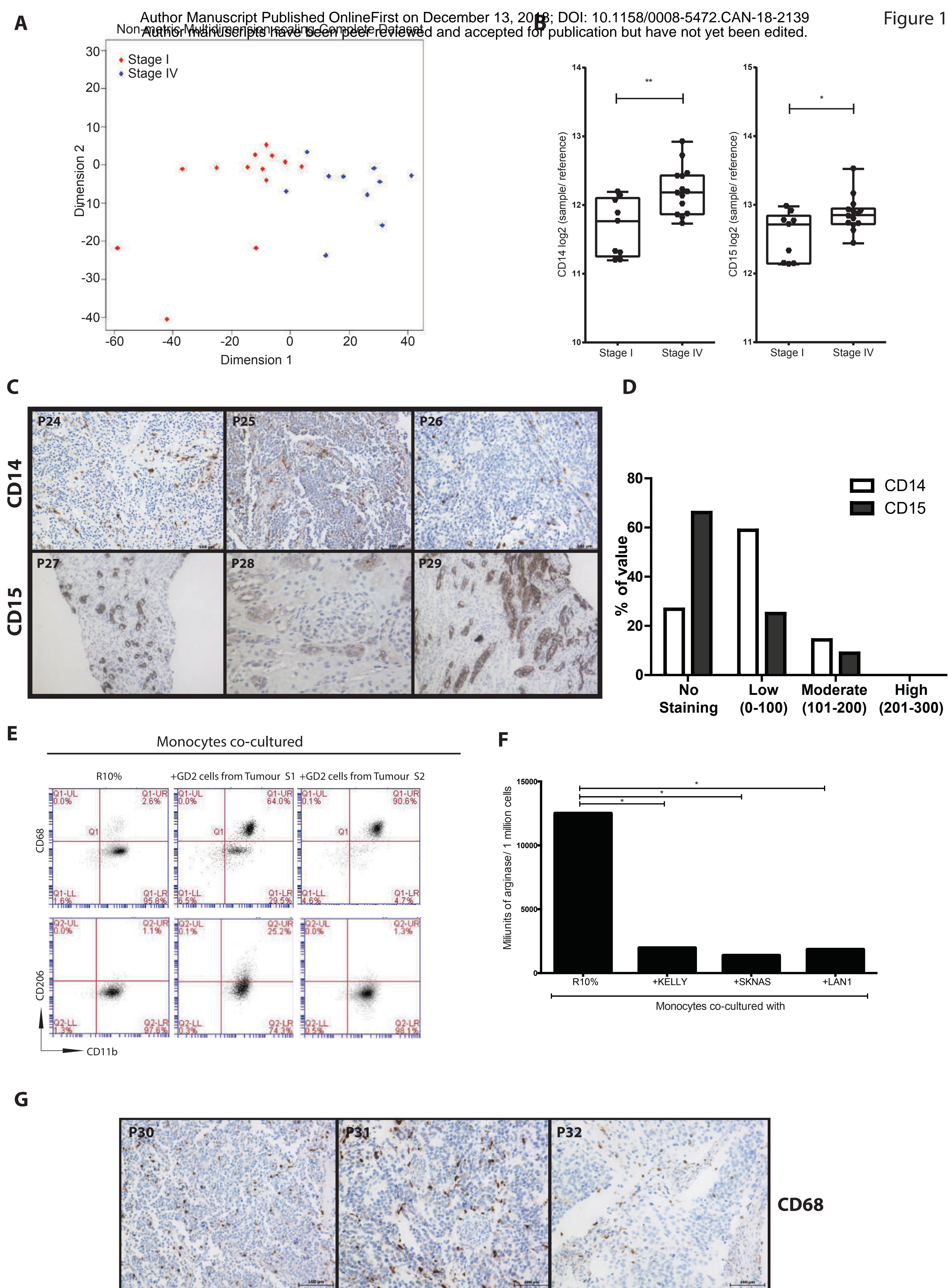

Downloaded from cancerres.aacrjournals.org on January 7, 2019. © 2018 American Association for Cancer Research.

Author Manuscript Published OnlineFirst on December 13, 2018; DOI: 10.1158/0008-5472.CAN-18-2139
Author manuscripts have been peer reviewed and accepted for publication but have not yet been edited.

Figure 2

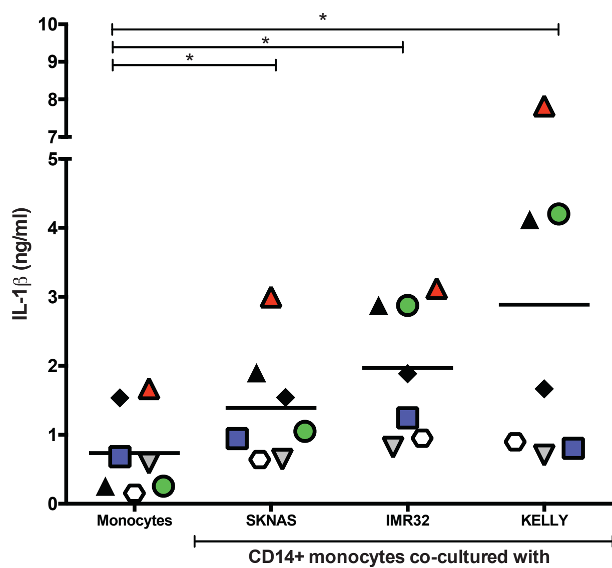

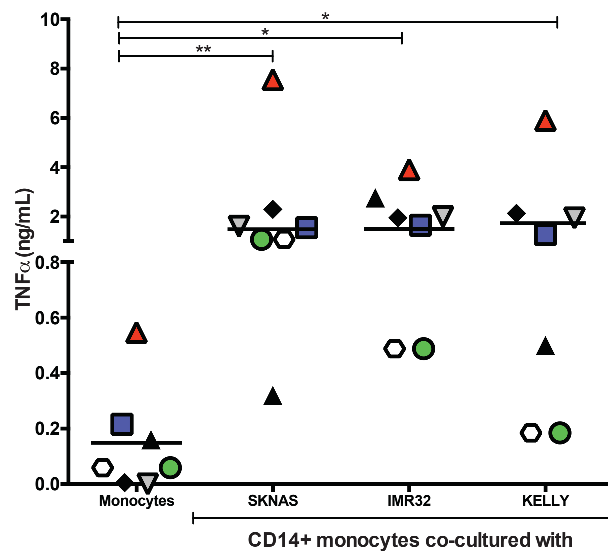

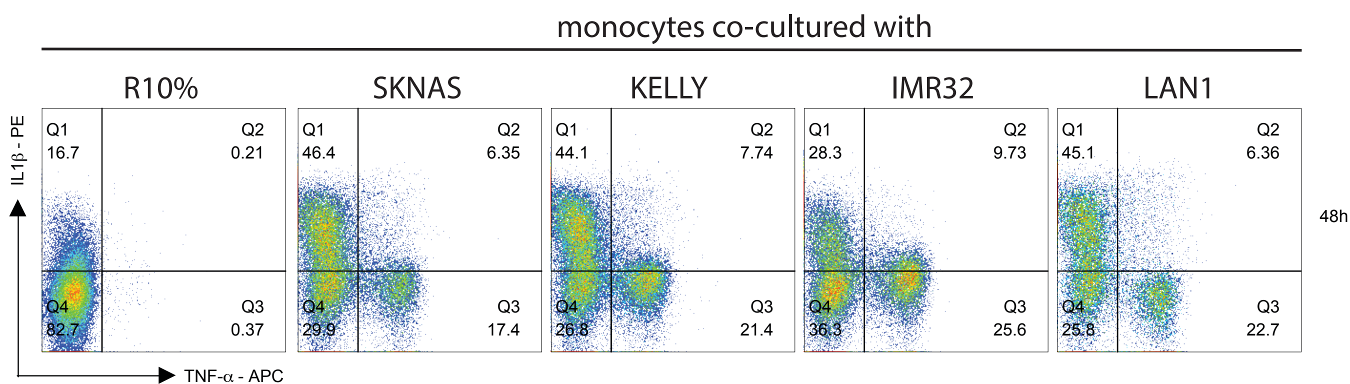

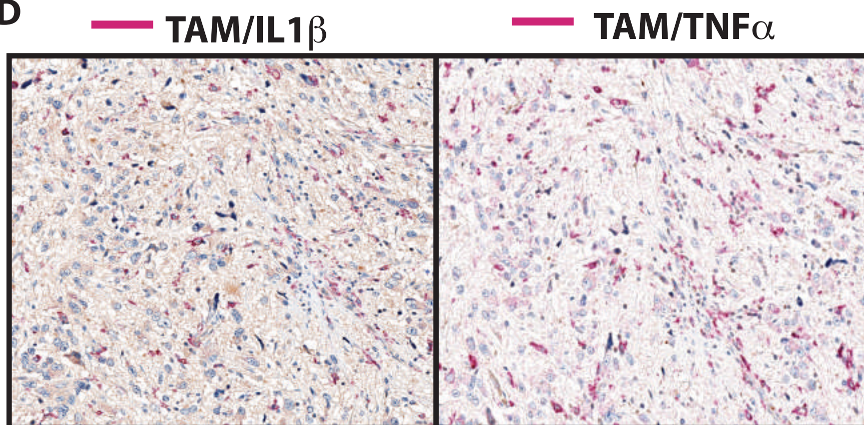

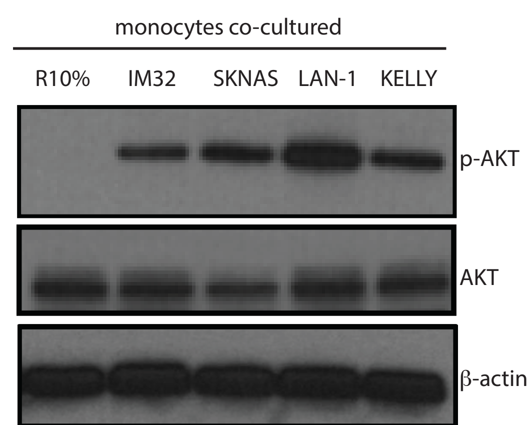

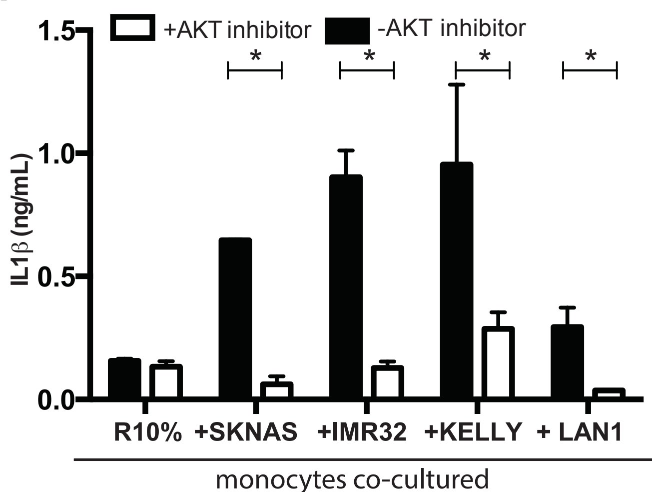

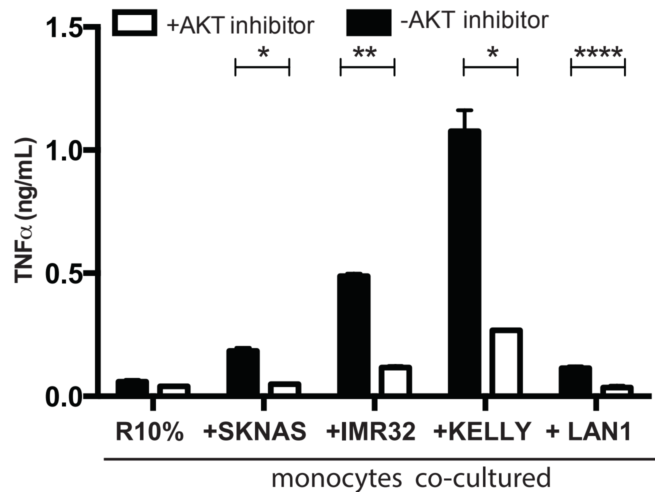

Downloaded from cancerres.aacrjournals.org on January 7, 2019. © 2018 American Association for Cancer Research.

Author Manuscript Published OnlineFirst on December 13, 2018; DOI: 10.1158/0008-5472.CAN-18-2139
Author manuscripts have been peer reviewed and accepted for publication but have not yet been edited.

Figure 3

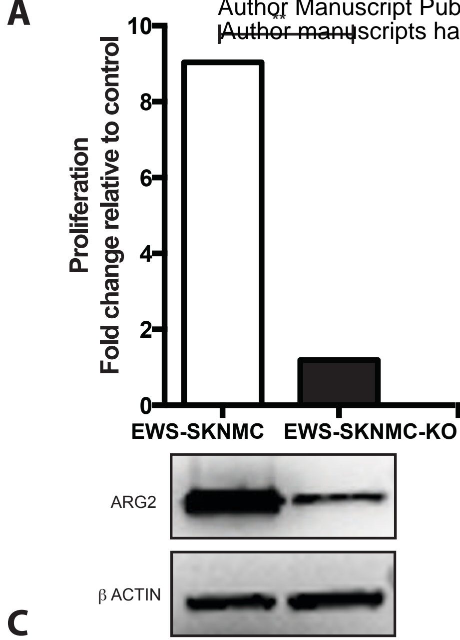

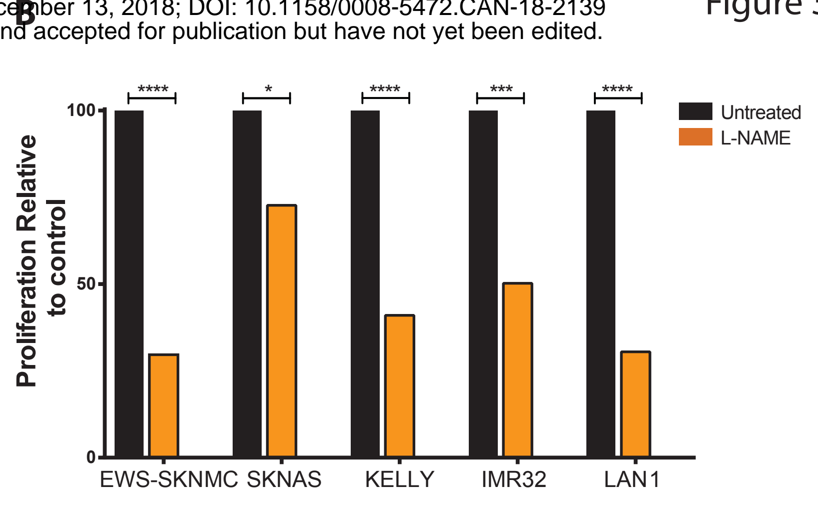

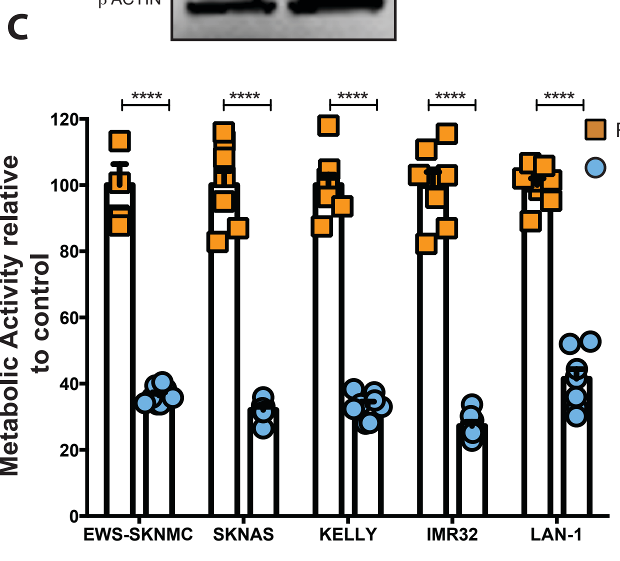

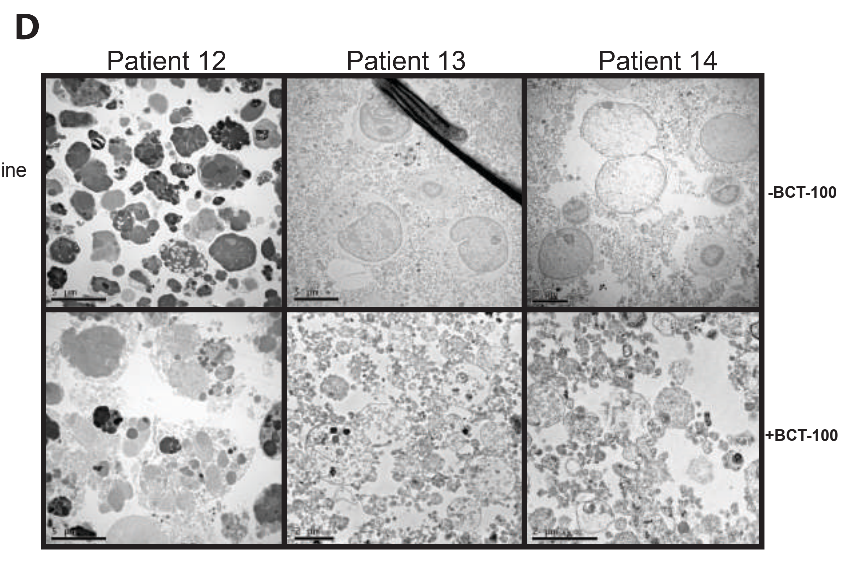

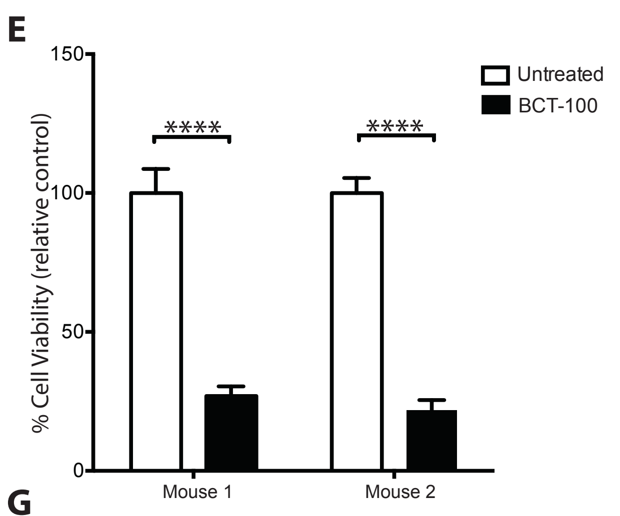

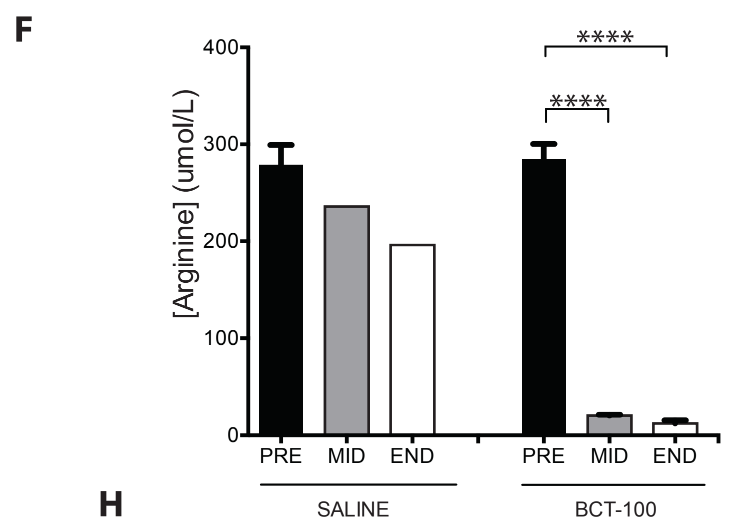

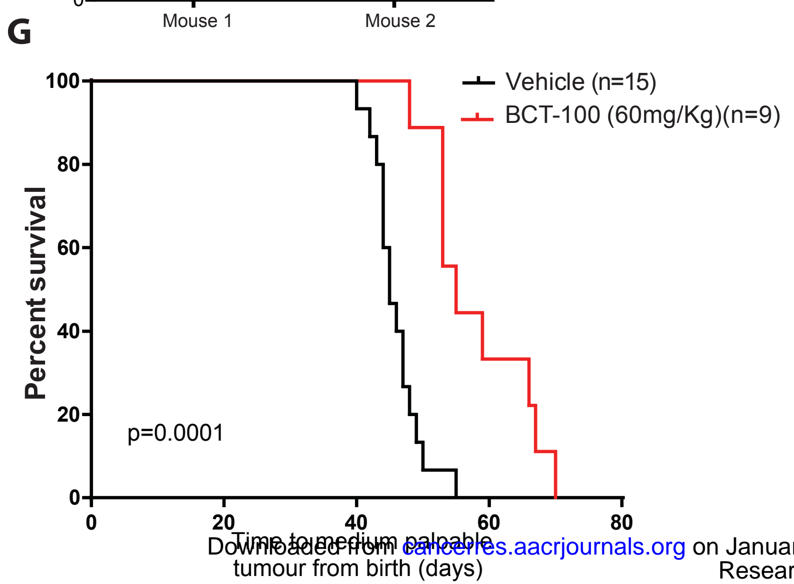

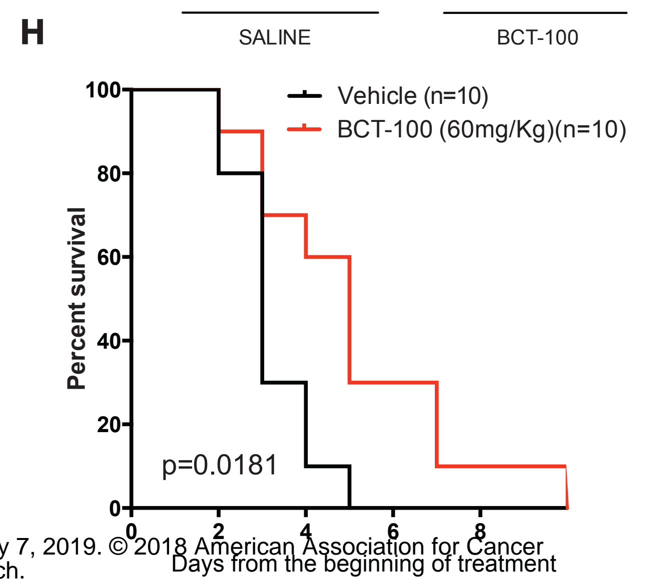

Downloaded from cancerres.aacrjournals.org on January 7, 2019. © 2018 American Association for Cancer Research.

Author Manuscript Published OnlineFirst on December 18, 2018; DOI: 10.1158/0008-5472.CAN-18-2139
Author manuscripts have been peer reviewed and accepted for publication but have not yet been edited.

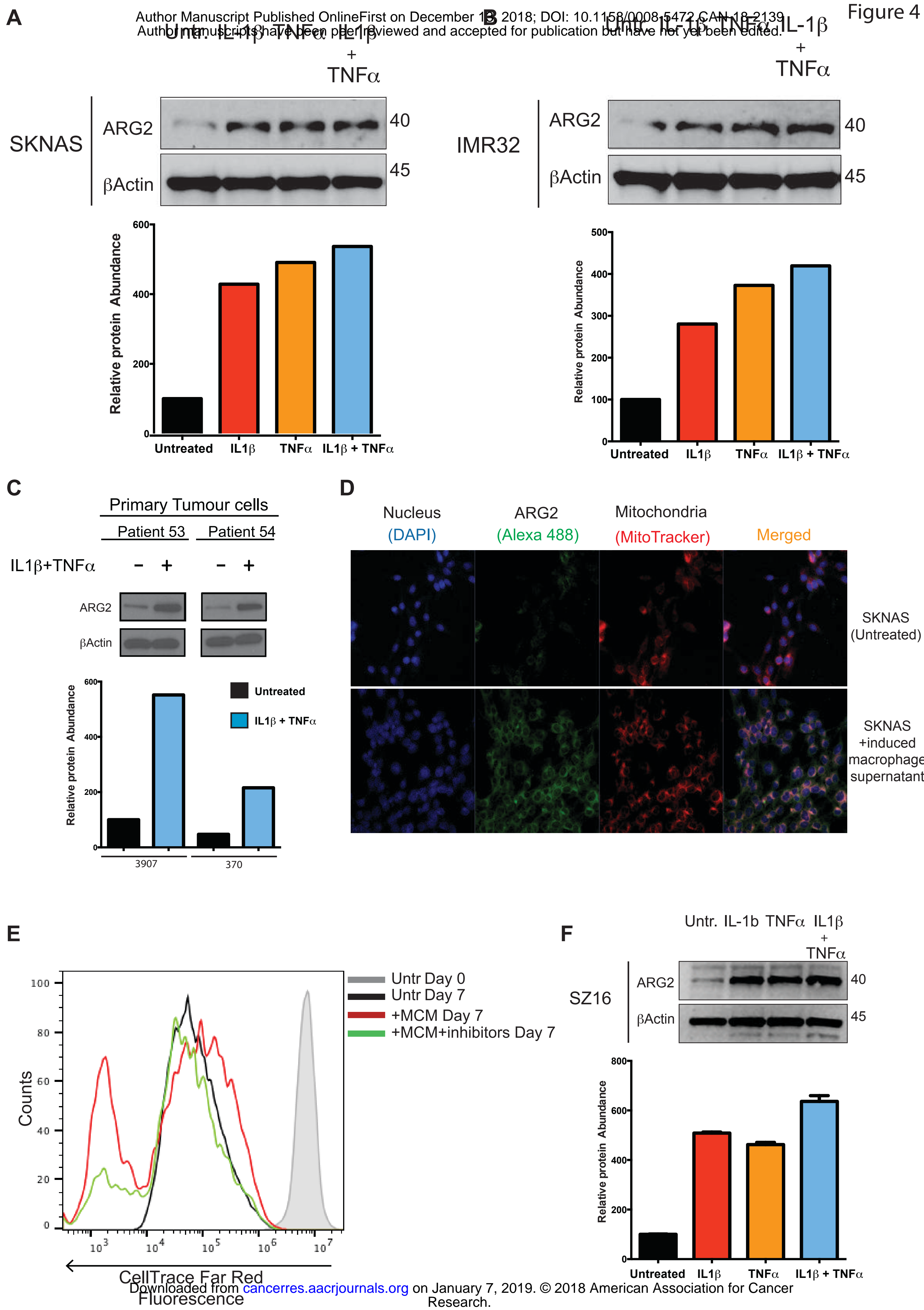

Downloaded from cancerres.aacrjournals.org on January 7, 2019. © 2018 American Association for Cancer Research.

Author Manuscript Published OnlineFirst on December 13, 2018; DOI: 10.1158/0008-5472.CAN-18-2139
Author manuscripts have been peer reviewed and accepted for publication but have not yet been edited.

Figure 5

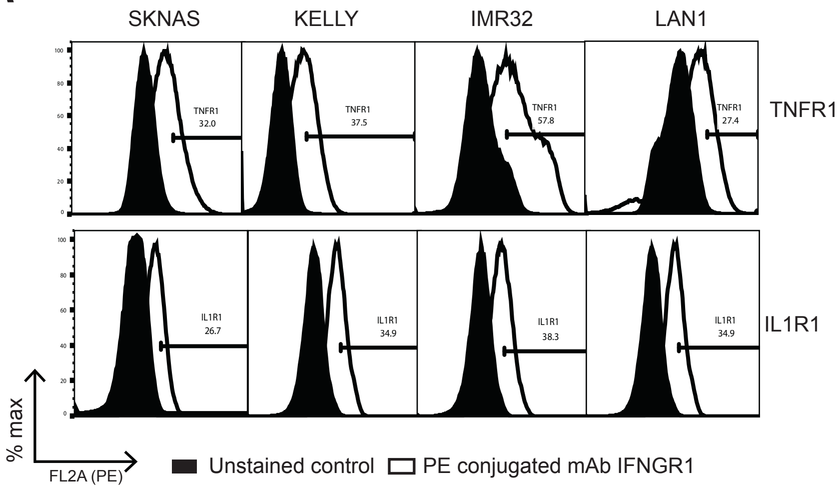

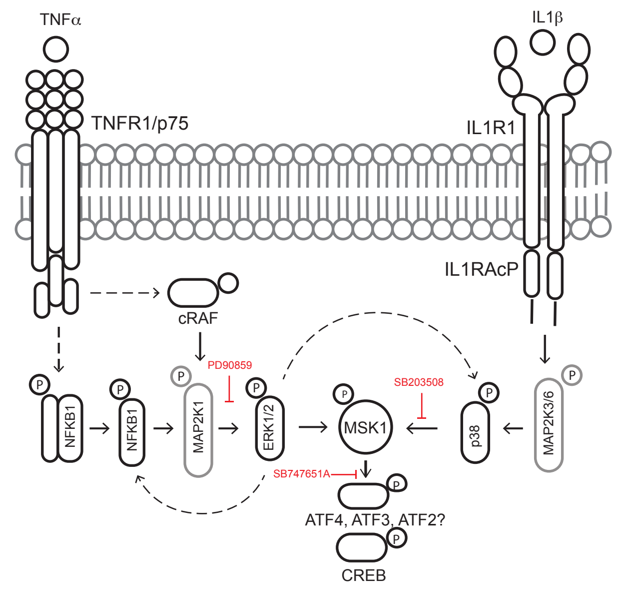

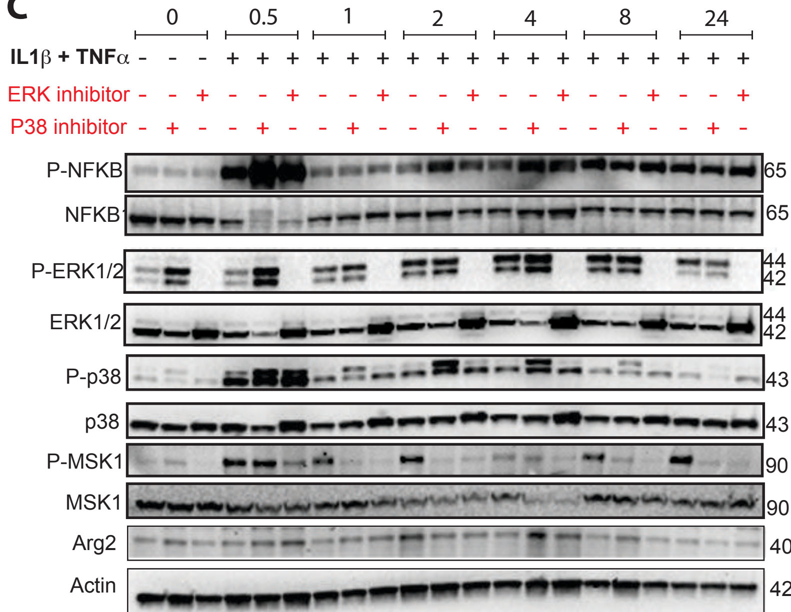

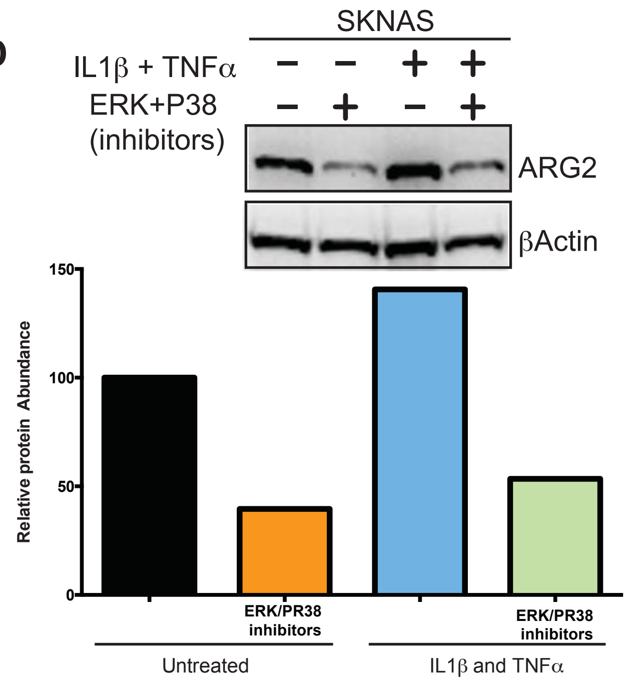

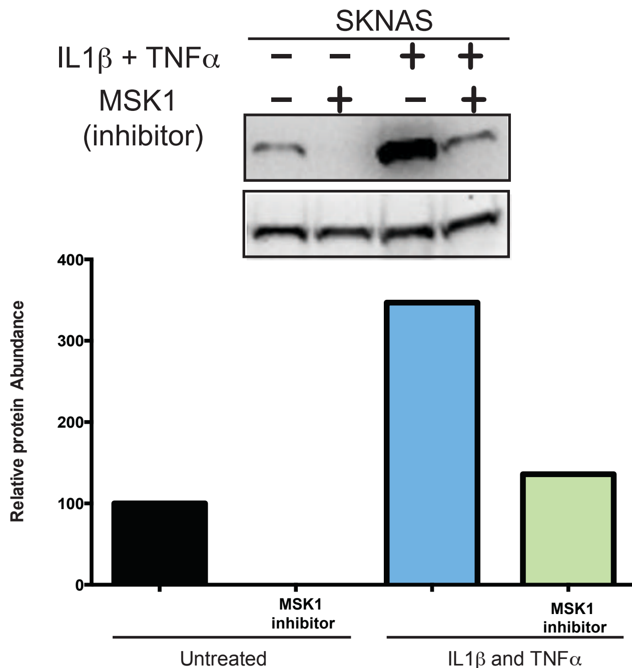

Downloaded from cancerres.aacrjournals.org on January 7, 2019. © 2018 American Association for Cancer Research.

Author Manuscript Published OnlineFirst on December 13, 2018; DOI: 10.1158/0008-5472.CAN-18-2139
Author manuscripts have been peer reviewed and accepted for publication but have not yet been edited.

Figure 6

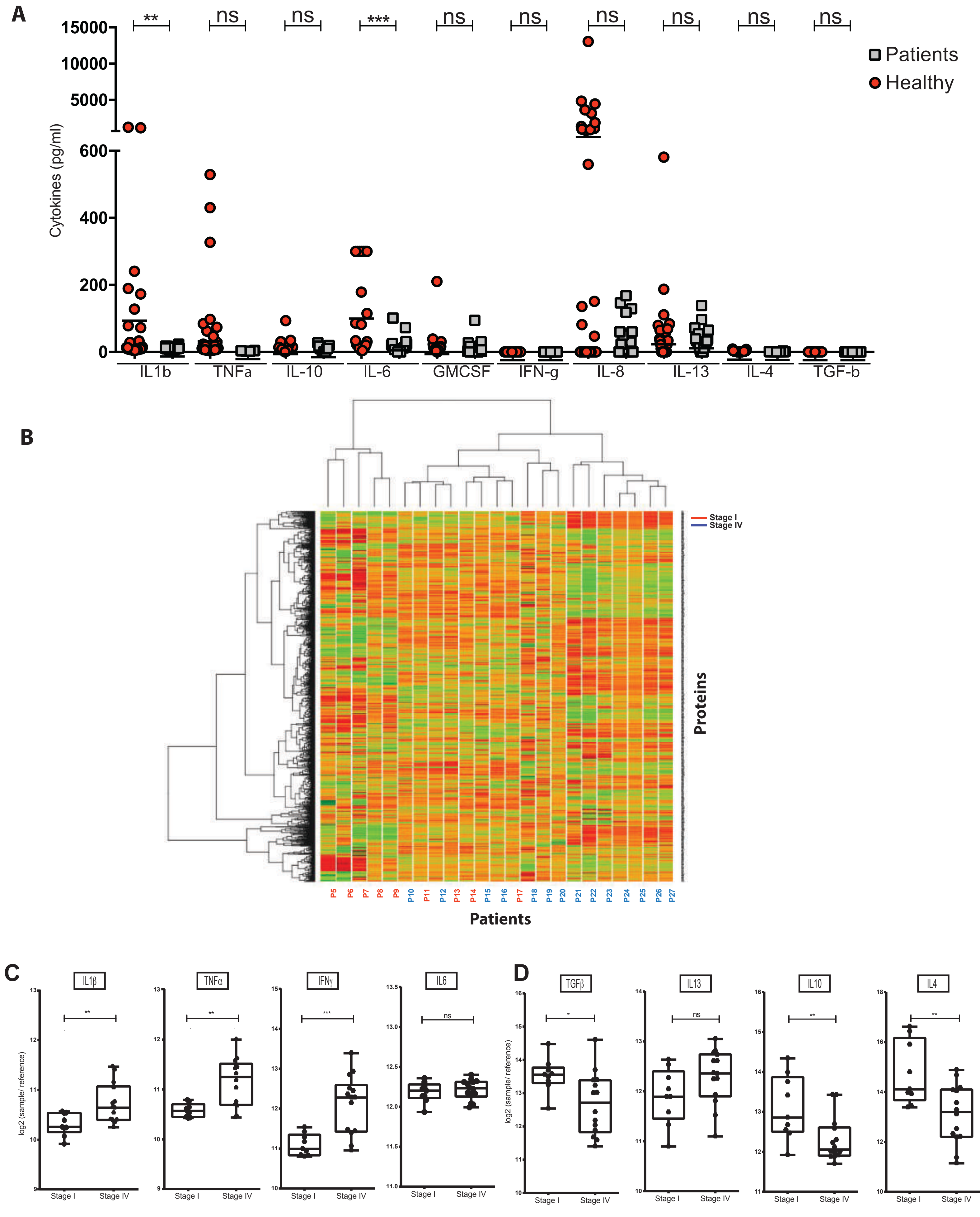

Downloaded from cancerres.aacrjournals.org on January 7, 2019. © 2018 American Association for Cancer Research.

Author Manuscript Published OnlineFirst on December 13, 2018; DOI: 10.1158/0008-5472.CAN-18-2139
Author manuscripts have been peer reviewed and accepted for publication but have not yet been edited.

Figure 7

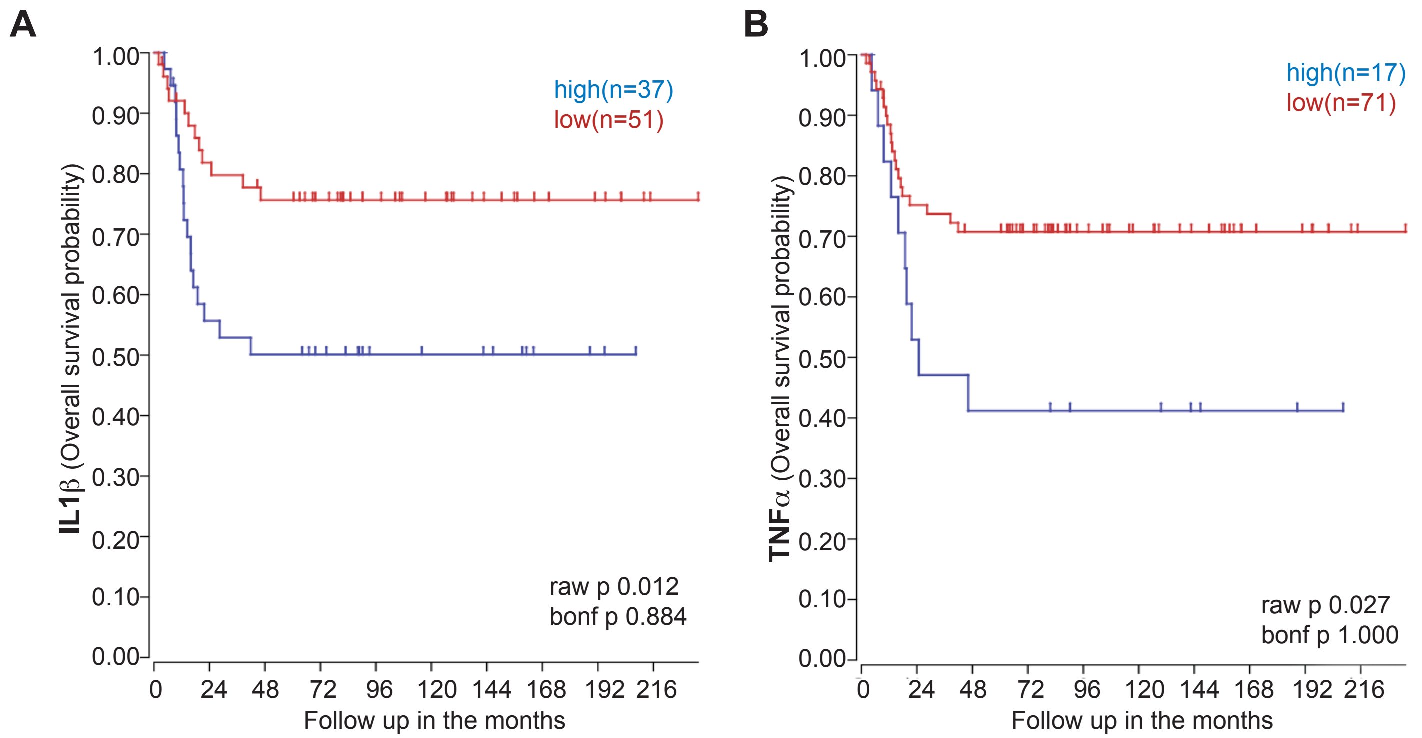

Downloaded from cancerres.aacrjournals.org on January 7, 2019. © 2018 American Association for Cancer Research.

Author Manuscript Published OnlineFirst on December 13, 2018; DOI: 10.1158/0008-5472.CAN-18-2139
Author manuscripts have been peer reviewed and accepted for publication but have not yet been edited.

Cancer Research
The Journal of Cancer Research (1916–1930) | The American Journal of Cancer (1931–1940)

AACR American Association for Cancer Research

Macrophage-derived IL-1β and TNF-α regulate arginine metabolism in neuroblastoma

Livingstone Fultang, Laura D Gamble, Luciana Gneo, et al.

Cancer Res Published OnlineFirst December 13, 2018.

Updated version	Access the most recent version of this article at: doi:10.1158/0008-5472.CAN-18-2139
Supplementary Material	Access the most recent supplemental material at: http://cancerres.aacrjournals.org/content/suppl/2018/12/12/0008-5472.CAN-18-2139.DC1
Author Manuscript	Author manuscripts have been peer reviewed and accepted for publication but have not yet been edited.

E-mail alerts	Sign up to receive free email-alerts related to this article or journal.
Reprints and Subscriptions	To order reprints of this article or to subscribe to the journal, contact the AACR Publications Department at pubs@aacr.org.
Permissions	To request permission to re-use all or part of this article, use this link http://cancerres.aacrjournals.org/content/early/2018/12/19/0008-5472.CAN-18-2139. Click on "Request Permissions" which will take you to the Copyright Clearance Center's (CCC) Rightslink site.

Downloaded from cancerres.aacrjournals.org on January 7, 2019. © 2018 American Association for Cancer Research.